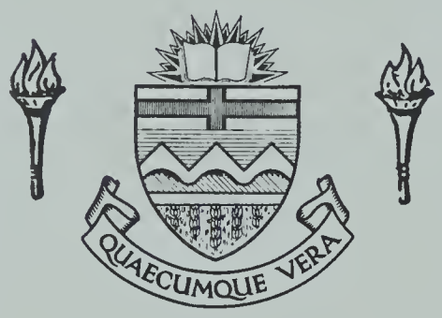

The University of Alberta
Printing Department
Edmonton, Alberta

THE UNIVERSITY OF ALBERTA

THE EFFECT OF A FREEZE-THAW CYCLE ON THE DRY BULK DENSITY OF A SOIL

by

ROBERT GEORGE CESSFORD

A THESIS

SUBMITTED TO THE FACULTY OF GRADUATE STUDIES

IN PARTIAL FULFILMENT OF THE REQUIREMENTS FOR THE

DEGREE OF MASTER OF SCIENCE

DEPARTMENT OF AGRICULTURAL ENGINEERING

EDMONTON, ALBERTA

FALL, 1970

UNIVERSITY OF ALBERTA

FACULTY OF GRADUATE STUDIES

The undersigned certify that they have read, and recommend to the Faculty of Graduate Studies for acceptance, a thesis entitled "The Effect of a Freeze-Thaw Cycle on the Dry Bulk Density of a Soil" submitted by Robert George Cessford in partial fulfilment of the requirements for the degree of Master of Science.

ABSTRACT

The primary purpose of this investigation was to examine one aspect of the compaction problem, viz. the effect of a freeze-thaw cycle on the bulk density of a soil. Moisture content, temperature (freezing rate) and initial density were parameters considered in the project. A moisture-density meter was designed and built for the purpose of measuring bulk density and moisture content non-destructively. Analysis of variance and multiple regression techniques were used to analyze the data. The following results and conclusions were obtained:

1. Non-destructive measurement of soil bulk density and moisture content was achieved using a dual energy gamma transmission technique.
2. Significant density changes were caused by an interaction of the parameters temperature x initial density.
3. Density changes due to the levels of the factors considered in the experiment were small, indicating little loosening of compacted soil during a freeze-thaw cycle.
4. Prediction of density responses in the field would not be possible on the basis of results obtained in this experiment.

TABLE OF CONTENTS

LIST OF TABLES . . . . . (i)

LIST OF FIGURES . . . . . (ii)

1. INTRODUCTION. 1

1.1 Basis for Study 1

1.1.1 Compaction 1

1.2 Objectives 2

2. REVIEW OF LITERATURE. 4

2.1 Soil Compaction 4

2.1.1 Mechanics of Compaction 4

2.1.2 Compaction by Vehicular Traffic 9

2.1.3 Effect of Cultivation 11

2.1.4 Minimum Tillage 11

2.2 Effects of Compaction 12

2.2.1 Mechanical Impedence 13

2.2.2 Aeration and Water Permeability 14

2.3 Frost Action on Soils 14

2.4 Measurement of Moisture and Density 17

2.4.1 Non-Destructive Methods 18

2.4.2 Gamma Transmission Techniques 20

3. THEORY 24

3.1 Nature of Gamma Radiation 24

3.2 Interaction of Gamma Radiation with Matter 26

3.3 Gamma-Ray Moisture and Density Detection 28

3.4 Principle of Dual Energy Transmission 30

3.5 Scintillation Detection 33

3.6 Radiation Protection 33

4. INSTRUMENTATION. 36

4.1 General Description of Moisture-Density Meter 36

4.2 Gamma Sources 36

4.3 Detection Equipment 38

4.4 Differential Discriminator 40

4.5 Counting and Timing Units 44

4.6 Probe Apparatus and Controls 49

4.7 Radiation Protection Equipment 52

5. PROCEDURES 54

5.1 Calibration 54

5.1.1 Optimum Gain versus High Voltage 54

5.1.2 Spectrum Calibration 55

5.1.3 Horizontal and Axial Alignment 57

5.1.4 Counting Standards 58

5.1.5 Preparation of Calibration Samples 58

5.1.6 Determination of Calibration Curves 59

5.2 Experimental Procedure 60

5.2.1 Experimental Design 60

5.2.2 Collection of Sample Material 62

5.2.3 Sample Preparation 63

5.2.4 Moisture-Density Measurement 65

5.2.5 Standardized Procedures 65

5.2.6 Freezing Procedure 67

5.2.7 Thawing and Re-Measuring 69

5.2.8 Data Processing 69

6. RESULTS. 71

6.1 Analysis of Variance 71

6.2 Multiple Regression 79

7. DISCUSSION OF RESULTS. 80

7.1 Analysis of Variance 80

7.2 Regression Analysis 82

7.3 Comments 82

8. CONCLUSIONS. 83

9. RECOMMENDATIONS. 85

10. BIBLIOGRAPHY. 86

11. APPENDICES 91

Appendix I 92

Appendix II 98

Appendix III 99

Appendix IV 101

LIST OF TABLES

TABLE	TITLE	PAGE
1	SOURCE SPECIFICATIONS	36
2	INSTRUMENT SETTINGS ESTABLISHED FOR AMERECIUM AND CESIUM SOURCES.	57
3	MASS ABSORPTION COEFFICIENTS FOR SOIL AND WATER AT TWO GAMMA ENERGIES.	60
4	EXPECTED VALUES OF THE MEAN SQUARES FOR A SPLIT PLOT MODEL IN A RANDOMIZED COMPLETE BLOCK DESIGN.	62
5	MEAN DENSITY CHANGE IN POUNDS PER CUBIC FOOT FOR THE FACTORS.	72
6	ANALYSIS OF VARIANCE FOR DENSITY CHANGE.	73
7	REGRESSION ANALYSIS RESULTS FOR DENSITY CHANGE. . . .	79

LIST OF FIGURES

FIGURE	TITLE	PAGE
1	ILLUSTRATION OF THE EFFECT OF MOISTURE CONTENT AND COMPACTIVE EFFORT ON DRY BULK DENSITY.	6
2	THE RELATION BETWEEN THE RATES OF ABSORPTION COEFFICIENTS FOR SOIL AND WATER AND GAMMA RAY ENERGY FOR TWO CONTRASTING SOILS (CALCULATED).	31
3	SCHEMATIC ARRANGEMENT OF COUNTING AND DETECTION SYSTEM.	37
4	SOURCE ASSEMBLY.	39
5	MODIFIED SCINTILLATION DETECTOR.	41
6	OPERATION OF A PULSE HEIGHT ANALYZER.	42
7	TYPICAL GAMMA ENERGY SPECTRUM SHOWING PHA WINDOW STRADDLING PRIMARY PHOTOPEAK.	42
8	PULSE HEIGHT ANALYZER CIRCUIT.	43
9	ELECTRONIC COUNTER IN C/B-A MODE.	45
10	COUNTING AND TIMING SYSTEM.	47
11	ELECTRONIC COUNTERS AND DIGITAL COMPARATOR.	48
12	LIFTING MECHANISM.	50
13	MICRO SWITCHES.	51
14	FILM BADGE AND SURVEY METER.	53
15	GAMMA RAY SPECTRA FOR AMERECIUM^{-241} and CESIUM^{-137} . . .	56
16	SOIL MIXER.	64
17	MODIFIED PROCTOR HAMMER.	64
18	SAMPLE IN MEASURING POSITION.	66
19	INSULATED SAMPLE CONTAINER.	68

FIGURE	TITLE	PAGE
20	THERMOCOUPLES INSTALLED IN SAMPLE TUBE.	68
21	GRAPH ILLUSTRATING TEMPERATURE AND INITIAL DENSITY INTERACTION.	74
22	GRAPH ILLUSTRATING TEMPERATURE AND MOISTURE INTERACTION.	76
23	GRAPH ILLUSTRATING THE EFFECT OF TEMPERATURE ON CHANGE IN DENSITY.	77
24	GRAPH ILLUSTRATING THE EFFECT OF MOISTURE CONTENT ON CHANGE IN DENSITY.	78

1. INTRODUCTION

1.1 Basis for Study

Soil is most often evaluated, in the field of agriculture, by the environment it provides for plant growth. Mechanized tillage can substantially alter this environment by changing the physical conditions of the soil which in turn affect mechanical support, mechanical impedence and supplies of air, water and heat. Unfortunately, these changes do not always improve the plant root environment[11].

More must be known about the ideal soil environment required by a crop as well as the complex phenomena in soil-machine systems if more realistic tillage objectives are to be defined. At the present time, a basic mechanics describing soil and plant behavior in comparable terms is not adequately developed[9].

1.1.1 Compaction

Compaction of the soil under wheels of power units and implements is an inevitable side-effect of current tillage operations and, as field equipment becomes larger and heavier, the harmful effects of soil compaction are of increasing concern. Large amounts of compactive energy are exerted by modern machinery and often this compaction extends several feet deep. New minimum tillage operations often till only the soil required for planting, greatly reducing tillage energy requirements. However, the soil is still subjected to compactive forces from the wheels of power units and other vehicular traffic. For example, consider a tractor equipped with 18.4 x 34 rear tires and pulling a 30 foot implement. A simple calculation will show that approximately 10% of the total field area will be subjected to the

compactive forces of the rear tractor wheels in a single tillage operation.

Regardless of the type of tillage practice it is evident that a significantly large amount of compactive force is exerted on the soil over a period of one or more cropping cycles. In fact, this situation has led to the suggestion that current tillage practices may be doing more damage to the soil in terms of plant requirements than nature can overcome[11].

1.2 Objectives

The purpose of this investigation was to examine one aspect of the compaction problem, viz. the effect of a freeze-thaw cycle on the bulk density of a soil. The following objectives were considered:

1. To implement a fast, accurate method of measuring bulk density and moisture content without destroying the sample. The instrument should be capable of a high degree of sample resolution (i.e. able to measure moisture and density in finite soil layers).
   Although this experiment was designed as a laboratory study, it was desirable that the instrument be capable of in-situ measurements for future field studies.
2. To calibrate and assess the accuracy of the instrument.
3. To develop experimental procedures suitable for a laboratory study on density including sample randomization and replication.
4. To investigate the influence of a set of independent variables on bulk density using statistical tools such as analysis of variance and regression analysis. The

independent variables were to include temperature (freezing rate), initial moisture content and bulk density.

2. REVIEW OF LITERATURE

2.1 Soil Compaction

Soil compaction has long been of interest to engineers in the design of foundations, road beds, earth fill dams and many other projects. More recently the agricultural engineer has become interested in the compaction of agricultural soils and its effects on seedling emergence and crop yields. On the following pages, papers are reviewed pertaining to the compaction of agricultural soils and methods of measuring and assessing compaction.

2.1.1 Mechanics of Compaction

Cooper and Nichols[11] define compaction as "the increasing of the soil bulk density by the reduction of pore space between the soil particles." They state that measurement of pressure alone gives no indication of the compaction resulting from the pressure. Compaction from a given pressure depends upon mineralogical and mechanical composition, moisture content, and the initial degree of consolidation. It was also concluded that compaction may be less for a static pressure than for a dynamic force (eg. slippage of a tractor tire).

Bekker[4], in a study of compaction, stated that mechanically the compaction of soils presents a difficult problem. Stress versus settlement relationships for a real soil cannot be expressed unequivocally. The empirical methods of study of the compression on soil reactions, which are based upon experiments such as the confined compression test, Atterberg test, and plastic limit test have little direct application in the case of vehicles or farm implements.

Chancellor and Schmidt[9] examined the effects of physical

phenomena at the soil surface, namely application of a pressure, displacement of a rut volume, and energy expended. The effects within the soil mass were soil movement, density increase (compaction) and dimensional soil deformation. Two soils were studied (a clay loam and a sandy loam) and the relationships between causes and effects were found to be influenced by:

a) soil type

b) moisture content

c) initial density

d) rut width and depth.

In unsaturated soils a large portion (70-100%) of the volume of surface impression was absorbed as compaction within the soil mass. This was concluded to be a distinguishing feature of agricultural soils as compared to soils of interest in foundation engineering.

Lambe[27] explained the theory of compaction with the following illustration (figure 1).

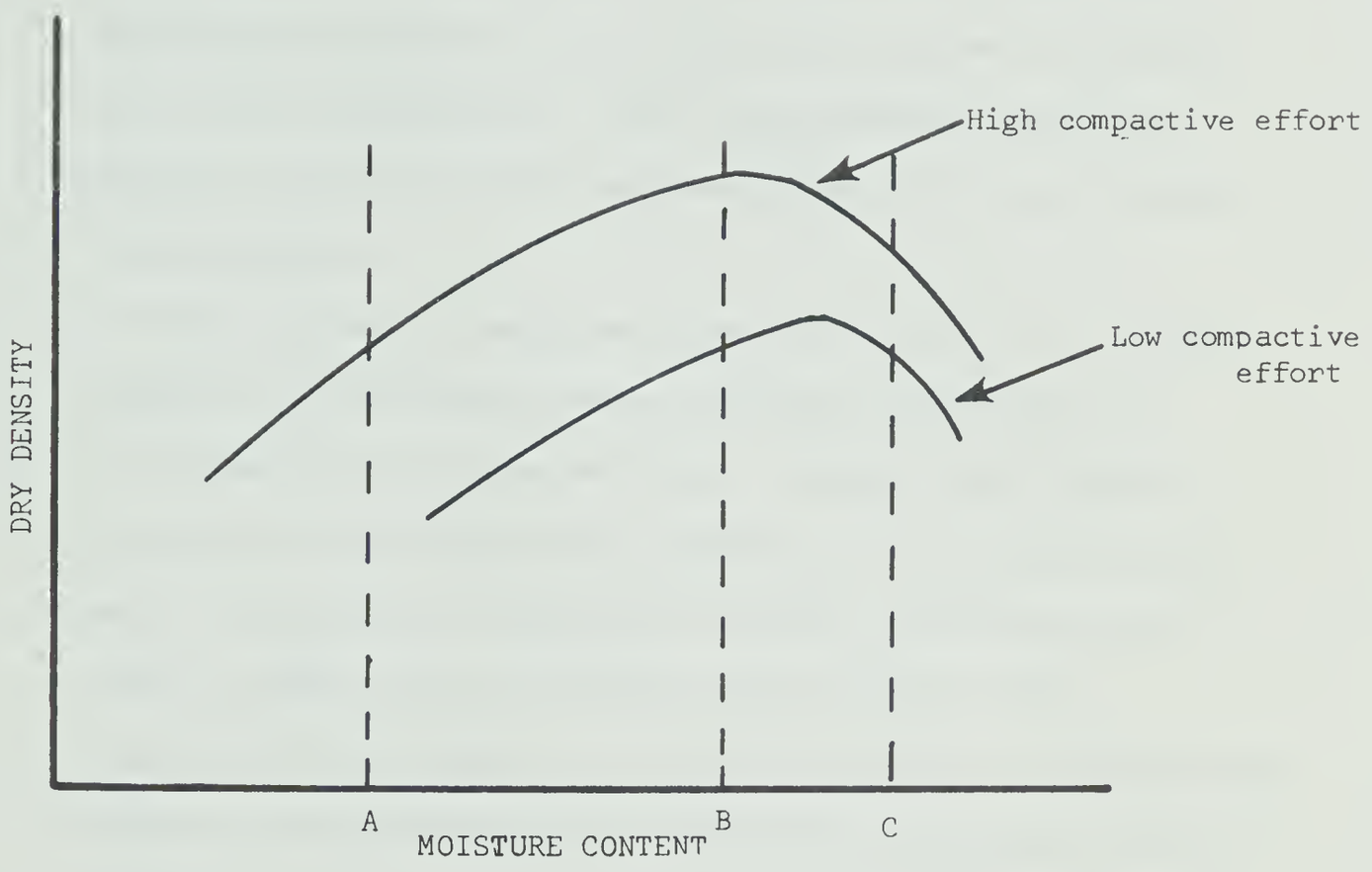

Figure 1: Illustration of the effect of moisture content and compactive effort on dry bulk density[27].

1. At A there is not enough water for the diffuse double layers of soil colloids to develop fully. Therefore, there is a low degree of compaction due to the high resistance of the highly viscous water.
2. Increasing water content from A to B expands the double layer around the soil particles and reduces flocculation by reducing electrolytic concentration. With this increased lubrication, particles are able to slide past each other into a more oriented and denser bed.
3. A further increase in moisture content to C results in a further expansion of the double layer and continued reduction in net attractive forces between particles. Although a more orderly arrangement of particles exists, density is lower because added water has diluted the concentration of soil particles per unit volume. Figure 1 also illustrates that a change in the compactive effort applied to a soil will result in a corresponding change in the moisture content at which the densest state will be reached.

Weaver and Jamison[60] studied moisture content versus tractor compaction relationships for two unconfined soils and compared these relationships with results obtained from modified Proctor procedures. It was found that peak compaction in both laboratory (Proctor) and soil bin tests became evident in the vicinity of the lower plastic limit which, according to Baver[3], is about the optimum moisture content for tillage.

Similarly, Bourget et al[6], in studies of tractor compaction on a clay loam, found that maximum compaction occurred at moisture

contents near the optimum plowing moistures. The optimum moisture content for compaction was found by the Proctor method to be 21 percent with a maximum dry density of 1.60 g cm^{-3}.

Gill[19] lists the following conditions during which soil is susceptible to compaction.

a) when the soil is loose

b) when the soil is wet and compressive strength is low

c) when the load is very heavy (depth of compaction increases with the size of the total load which applies the compacting forces).

d) when repeated loads are applied. (90 percent of compaction is obtained with the first pass of a vehicle. Therefore, repeated loading would have the effect of compacting a greater proportion of the total area rather than increasing the degree of compaction at a specific site).

In a study of the effects of time on compaction, Alboaba[1] found that compaction of soil by a roller was reduced as speed was increased. This was attributed to the time factor (i.e. the period of time the roller was in contact with the soil and was available to exert its weight). Similarly, Vomocil et al[57] found that compaction caused by tractor wheels was reduced at higher speeds. However, in comparison with moisture content, the effect of speed was quite unimportant. In fact, the reduction in compaction caused by increasing the speed from one to twelve miles per hour was the same as that caused by a one percent reduction in moisture content.

2.1.2 Compaction by Vehicular Traffic

Many investigators have studied the effects of vehicular traffic on the physical properties of soils and it is generally agreed that the major effect is compaction or increase in bulk volume weight.

Weaver[59], as a result of laboratory tests on a loam soil with an 11 - 38 tractor tire loaded to 2185 pounds, concluded that "the farm tractor may be regarded as a potential contributing factor in the formation of subsurface hardpans." Similarly, Doneen and Henderson[13] stated that "compaction is widespread in California - apparently the result of tractors and other heavy farm equipment."

Gill[19] stated that soil compaction was increasing due mainly to the following factors:

a) increases in weight, speed and power of machinery in crop production

b) increasing amount of traffic or actual number of trips over the soil.

He concluded that forty years of cultivation in prairie soils of Ohio resulted in an increase of 20 percent in soil density and a decrease in the porosity of 10 percent.

Domier[12] stated that soil under tractor drive wheels is subject to compression forces (tractor weight) and shear forces (slippage). The main immediate effect of these forces is consolidation (increase in bulk density). In treatments using a 7000 pound tractor, it was found that bulk density increased with the first rolling but no significant increase was detected as the number of rollings increased. Penetrometer resistance, on the other hand, increased with the number of rollings.

Wheel traffic effects were studied by Feldman[16] and it was found

that neither soil compaction nor crop growth correlated with the amount of tractor wheel slip. Therefore, it would appear that compression force is the most important force in compaction by wheeled vehicles.

Evidence has been presented indicating that compaction developed by wheel traffic extends far below plow depth and is not removed by subsequent tillage operations[49]. Weaver[59], while investigating tractor compaction on a loam soil, found that annual tractor usage was capable of compacting to a depth of nine inches when moisture content was near optimum (11 - 15 percent). As a result of compaction studies on irrigated soils, Doneen and Henderson[13] suggest that tractor compaction may extend to depths of up to 20 inches.

Traffic soles (compaction observed below the cultivated layer) have also been studied by Free[17] and Baver[3]. Free found that, for a loam soil, the volume weight at the 10 - 13 inch depth was greater in wheel middles than in non-wheel furrows.

Vomocil and Flocker[56] concluded that the soil physical condition after compaction depends on many variables including the characteristics of the load applied as well as the characteristics of the soil at the time of compaction.

Vandenberg and Gill[52] studied pressure distribution between a smooth tire and the soil on the hypothesis that stresses occurring between a tractive device and soil determine the amount of soil compaction which may result. It was found that pressure distribution under a thin walled smooth rubber tire on a firm surface cannot be considered equal to the average pressure over the entire area of contact. With an inflation pressure of 14 psi, peak pressures of up to 32.5 psi were found at the periphery of the contact area. This factor must be taken into account in any study of tire-soil relationships for agricultural vehicles.

2.1.3 Effect of Cultivation

Investigations of various tillage treatments have shown that such practices have differing effects on soil bulk density. Van Doren et al[53] applied two surface treatments (tire compaction and disking operations) to a silty clay loam and measured the resulting bulk density and penetrability. Of the two types of surface compactive effort, surface tools contributed less toward compacting than did tires.

Bourget et al[6] found that on a clay loam, summerfallow and cropping treatment did not produce significant differences in bulk density and porosity.

Luttrell et al[29] applied treatments consisting of different combinations of plowing, disking and harrowing and studied the effects of these operations on bulk density, clod size, and surface roughness. Plowing reduced bulk density by approximately 25 percent while secondary tillage operations tended to increase the bulk density. However, the differences in bulk density caused by secondary tillage operations were not significant.

2.1.4 Minimum Tillage

Swamy Rao et al[48] studied the effects of minimum tillage on the physical properties of two soils, a clay loam and a silty loam. Comparison of minimum tillage with conventional methods showed that the minimum tillage treatments resulted in a lower soil bulk density and less resistance to penetration. The decreased amount of compaction was attributed to the lower amount of tractor and implement traffic on the minimum tillage plots.

Bowers and Bateman[7] compared the effects of minimum tillage and conventional tillage practices on yields of corn. Conventional tillage

provided excellent germination and early growth but compaction from excessive tillage reduced aeration and water intake for the growth stage immediately prior to tasseling. Compaction effect was most pronounced on clay soils where less compaction from minimum tillage gave a yield advantage in some cases. Similarly, Johnson and Taylor[23] found that stands and crop response on a clay soil were damaged by compactive effort from a soil packer or seed press wheel on fall plowed treatments. It was concluded that extra tillage operations are of little or no benefit.

2.2 Effects of Compaction

Since the basic mechanics describing compaction effects on crop response is not available[16], many empirical studies have been undertaken. The effects of compaction on crop response may be broadly divided into two categories; first, effects of mechanical impedence and second, effects of changes in aeration, soil temperature, infiltration capacity, and permeability to water. Phillips and Kirkham[39] state that it is difficult to show which property or properties affect plant growth since compaction influences many physical properties. There are relatively few quantitative data in the literature which clearly point out the exact mechanism by which soil compaction reduces plant growth.

Bourget et al[6] compacted a clay loam to four levels of density and studied oat yields. Oat yields on uncompacted plots were highly significantly greater than all others. However, yield differences on plots with 8, 14, 20 and 26 passes with a 6,000 pound tractor were not significant. These results are in accordance with the findings of Gill[19] and Domier[12] who concluded that a very large percentage of compaction is achieved with the first pass of a tractor wheel, while

subsequent rollings produce little additional density increase.

2.2.1 Mechanical Impedence

Morton et al[33] devised a method for measuring the force and energy exerted by a mechanical seedling. The energy required for emergence increased markedly with increasing compaction pressure at the soil surface. In a further experiment involving seedling emergence under simulated field conditions, it was found that applying a surface compaction pressure in excess of 1/2 psi suppressed seedling emergence. Similar results were obtained by Stout et al[47] in a soil bin experiment with a sandy clay loam. The effect of compaction on emergence varied directly with soil moisture content.

Phillips and Kirkham[39] found that mechanical impedence as measured by bulk density and needle penetration was the property which correlated most highly with the reduction in growth and yield of corn. However, this did not prove that mechanical impedence was the only factor involved.

Eavis[15] used time-lapse photography, penetrometer measurements, and an apparatus for measuring root reaction forces in a study of pea seedling roots. Both soil moisture tension and the soil bulk density affected mechanical impedence whether this was measured by the root method or with the penetrometer. Length, weight and volume of vacuolated cells of the pea root were approximately inversely proportional to the level of mechanical impedence.

Veihmeyer and Hendrickson[54] investigated sunflower root penetration on a number of soils with widely different water-holding characteristics at varying levels of density. High density soils were found to prevent penetration by roots. The density above which roots

did not penetrate was not necessarily the same for all soils, but no roots were found at densities of 1.9 g cm^{-3} or greater in any of the soils.

2.2.2 Aeration and Water Permeability

Bateman[2] evaluated crop response on two soils (silty clay loam and silt loam) as affected by machine operations. Factors considered to be of importance were moisture, temperature, aeration and mechanical impedence. Compaction caused significant yield decreases on silty clay loam but only a limited number of decreases on silt loam. On the highly compacted plots, air voids at field capacity were near the 10 percent level which was considered to be critical for corn.

Doneen and Henderson[13] found that water penetration was decreased due to compaction. At low apparent densities a small increase in the density resulted in a marked decrease in infiltration rate, while at high densities a relatively large increase in density caused only a slight further reduction in infiltration rate.

2.3 Frost Action on Soils

Relatively little quantitative information is available on the effect of frost action on the bulk density of agricultural soils. Kohnke[24] reviewed some of the general effects of soil freezing and thawing as summarized in the following four paragraphs.

The effect of ice formation upon soil structure depends on the moisture content of the soil, the pore size distribution, and the velocity of freezing. Little effect can be expected upon soil structure if the soil is nearly dry. Slow cooling and freezing of a moist soil results in the water freezing in the larger cavities where it is under the least tension. In the vicinity of the ice crystals the soil becomes drier and water will move toward these drier regions due to the tension gradient and diffusion. More water will freeze around the original ice

crystals and this process will continue until all "free" water is frozen, unless temperature changes have occurred. This water movement in the soil is influenced greatly by texture.

In a sandy soil, the pores are so large that water is under very little tension and freezes as soon as the temperature has dropped to 0°C. Since most pores are not completely filled with water before freezing, the nine percent expansion of water can be accommodated without substantial rearrangement of the solid particles. The result is a very slight loosening of the structure.

In a loam soil, however, the situation is quite different due to a much higher capillary conductivity. In the fine pores the water is held under high tension so that its freezing temperatures lie considerably below 0°C. As the 0°C isotherm descends into the soil, water in the large pores freezes. The liquid water in the capillary pores below this line moves up to the ice layer, increasing its thickness. The thickness of these ice lenses depends largely upon the velocity of freezing. When freezing is fast, ice lenses are thin, since the temperature in the soil below the lense quickly drops to a point where capillary movement is stopped.

Freezing of water in a clay has a particularly interesting effect on soil structure. The natural phenomena are similar to those in a loam. The pores in clay, however, are much finer and consequently capillary movement is much slower and the water is held at a higher tension. In addition, clay shrinks upon removal of water. The upward movement of water to the ice lense results in shrinking of the soil substance. The resulting cracks are large enough that water freezes in them at very nearly 0°C.

Limited experimental evidence has been presented which suggests that freeze-thaw cycles affect the bulk density of agricultural soils. Luttrell et al[29], in a study of the effect of certain tillage operations on bulk density and other soil properties, discovered that over-wintering caused a greater bulk density reduction than any of the tillage operations. A simular conclusion was reached by Kucera and Promersberger[25] who artificially compacted soils in several areas of North Dakota. It was found that a winter of freezing and thawing relieved artifically compacted layers so that no abnormal compaction could be detected.

The mechanism of freezing in soils and its effect on foundations, highways and other structures has been investigated. The results of this work may also be useful in describing frost action in agricultural soils.

Williams[61] concluded that frost heaving is caused by development of layers or lenses of ice, much larger than pore size, by migration of water to the frost line and its accumulation there as ice. Evidence was cited of migration of water into the frozen layer in an unsaturated soil. It was also found that certain soils when unsaturated undergo shrinkage on freezing. Ice crystals develop in air-filled voids and are fed by diffusion of vapor from the smaller capillary pores of the matrix. The loss of water from the matrix pores results in contraction of the material.

Penner[37] showed that a slow penetration of the frost line gives a higher concentration of ice in the frozen layer than a fast penetration. It was also found[36] that ice lenses in natural soil are normally found in a thermal gradient regime, and this permits the development of an undulating frost line if a range of pore sizes exists. Experimental results support the use of particle size as a valid basis for assessing frost susceptibility since smaller (capillary) pores are involved in the development of ice lenses. However, there does not appear to be an

abrupt dividing line based on particle or pore size that separates frost-heaving soils from non frost-heaving soils[35].

2.4 Measurements of Moisture and Density

Many methods are available for measuring the degree of soil compaction. Some of these techniques include the core method, sand cone, water displacement, penetrometer and radiation equipment.

Doneen and Henderson[13] found that water penetration was reduced due to compaction. The reduction in the rate of water infiltration was governed by the number of passes made by a tractor. Similarly, Vomocil et al[57] used infiltration rate as the main index of compaction in a study of the compacting effect of tractor wheels on a fine sandy loam. It was concluded that infiltration rate was a more sensitive measure of compacting effect than bulk density.

Vomocil and Flocker[56] reason that an increase in bulk density means a change in pore size distribution towards a smaller proportion of the coarser pores. Therefore, the determination of pore size distribution would be a useful measure of soil compaction.

A relatively popular tool for measuring compaction is the core sampler. Jamison et al[22] used sample cores to study tractor tire compaction effects in Cecil clay. Depth of penetration of compactive effects, maximum bulk density, and pattern of compaction were determined by this method.

The cone type penetrometer is another instrument which has been used widely in soil compaction and crop emergence studies[17,25,39,49]. Feldman[16] measured bulk density, soil shear strength, oxygen diffusion rate and cone penetrometer resistance in an investigation of wheel traffic effects. The penetrometer was found to be the most sensitive

and useful apparatus for field measurements, although readings varied somewhat with soil moisture content.

Both the penetrometer and core sampler have the disadvantage of destroying the part of the sample which is being measured. When a measurement has been made at a particular position with one of these instruments, it is not possible to take subsequent readings at precisely the same location.

2.4.1 Non-destructive Methods.

Density and moisture content of compacted soils have also been measured non-destructively by the use of radiation techniques. Vomocil[55] investigated the in situ measurement of soil bulk density by gamma ray absorption. The system was based on the absorption of gamma rays as a logarithmic function of the wet bulk density so that

$$\frac{I}{I_o} = e^{-\sigma dx} \quad \ldots\ldots\ldots\ldots\ldots\ldots\ldots\ldots\ldots\ldots (2.1)$$

where I_o = initial intensity of the radiation beam

I = intensity of the reflected radiation

x = thickness of the soil

σ = mass absorption coefficient

d = wet bulk density.

The instrument consisted of a double probe with the source (^{60}Co) and detector (Geiger-Mueller) being twelve inches apart. No electrical discrimination was used and all gamma rays reaching the detector, regardless of their energy, could be counted.

Phillips et al[38] used commercially available radiation equipment for plow-layer density and moisture determinations. The density probe consisted of a gamma radiation source and a Geiger-Mueller detector. The

source and detector were separated from each other by lead shielding. When the instrument was in use, gamma radiation was reflected back from the soil particles to the detector. The amount of reflected radiation depended largely upon the density of the soil. The sphere of influence (i.e. volume of soil which reflected the radiation) for this instrument was three to eight inches depending upon the density. A necessary assumption in the use of this instrument was that the density and moisture content were uniform to the depth in the soil to which the sphere of influence reached. Such uniformity did not exist. The overall precision of the method was found to be ± 0.06 g cm^{-3}.

Gurr[20] examined the use of gamma rays in measuring the water content in unsaturated columns of soil. The method was based on the assumption that scattering and absorption of gamma rays were related to the density of matter in their path. The major process involved is the reduction of the gamma quanta energy by Compton scattering. The number of gamma ray quanta per unit time recorded by a counter may be expressed as:

$$N = N_o e^{-x(\mu_s Pa + \mu_w C)} \quad \ldots\ldots\ldots\ldots\ldots\ldots (2.2)$$

where N_o = number of counts with no absorption

x = length of soil column (cm)

μ_s = mass absorption coefficient of soil particles ($cm^2 g^{-1}$)

μ_w = mass absorption coefficient of water ($cm^2 g^{-1}$)

Pa = bulk density of soil (g cm^{-3})

C = water content of soil (g cm^{-3})

For a given radioactive source, μ, and μ_w are fixed. To use this method for soil density determination, water content must be known and remain unchanged. Conversely, the method can be used for moisture determination if soil density is known and remains constant.

A method for determining soil moisture by neutron scattering was investigated by Stone et al[46]. Fast neutrons from a source were slowed down by hydrogen atoms in the soil water and the slowed neutrons were counted by a detector. Calibration of the probe was achieved by using gravimetric moisture data. It was found that readings were not satisfactory within six to twelve inches of the soil surface due to the escape of neutrons from the soil mass.

Pierpoint[40] attempted to improve the accuracy of the neutron probe in the top twelve inches by using a two inch polyethylene shield at the soil surface to prevent the escape of neutrons. It was found that a calibration could be made and that reasonably accurate readings could be achieved at the 6 inch depth. However, the instrument was not capable of measuring moisture content in finite layers of soil.

2.4.2 Gamma Transmission Techniques

Van Bavel et al[51] investigated the gamma transmission method for measuring soil density. Basically, the transmission method consists of locating a source of gamma radiation in the soil and measuring the radiation intensity at a fixed horizontal distance from the source. The radiation intensity when the source is placed in a material is subject to the following law:

$$I_x = I_o \{\exp^{-(\lambda_u x)}\}/x^2 \quad \ldots\ldots\ldots\ldots\ldots (2.3)$$

where I_o = radiation intensity at the source

I_x = radiation intensity at distance X from the source

λ_μ = linear attenuation coefficient (cm^{-1})

The coefficient $\lambda\mu$ is a characteristic of the material and the wave length of the radiation. Also,

$$\lambda\mu = \lambda\mu_o d \quad \ldots\ldots\ldots\ldots\ldots\ldots\ldots\ldots\ldots (2.4)$$

where $\lambda\mu_o$ = the mass attenuation coefficient ($cm^2 g^{-1}$)

d = density of the material ($g\ cm^{-3}$)

It was shown that the above equation pertains only to radiation of one wave length (primary radiation) and that absorption and scattering of radiation by the soil causes the measured intensity at the detector to be higher than predicted. A single channel pulse height analyser was used to exclude scattered or secondary radiation.

A further study by Van Bavel[50] showed that the resolution of the method was approximately 1/2 inch (i.e. density measurements could be taken in 1/2 inch layers of soil). The least significant differences that could be measured were about 0.01 gm cm^{-3}. It was found that the principal difficulty with the method was in the determination of moisture content by which dry bulk density was calculated. Moisture could be measured non-destructively by the neutron method but the respective resolutions did not match.

McHenry[30] used the gamma transmission method to measure the density of sediments. Performance of the dual probe was compared with a single probe (reflection method) in field operation. It was found that the scintillation detector which was used in conjunction with the dual probe was highly dependent upon the high voltage applied. Frequent adjustments of the high voltage gain control were necessary to maintain proper sensitivity and precision. However, the dual probe was able to measure density in narrow bands while the single probe was not.

McHenry and Dendy[31] assessed the accuracy of the dual probe

(transmission) method and found that the unit was capable of measuring the density of sediments to within 0.01 absolute density units. In a field test, sediment weights computed for a silt box on the basis of dual probe density measurements varied less than one percent from the gravimetric determination. Vertical resolution of less than one inch was achieved.

Lal[26] used the gamma transmission method in a laboratory study to determine the effect of packers on soil density and moisture loss. Based upon the theoretical analysis of gamma transmission, a linear relationship was found between the count rate and the moisture content, and between the count rate and the dry bulk density.

Difficulties associated with the gamma transmission method were pointed out by Ligon[28] as a result of a study of water balance and evapotranspiration. Commercially available equipment was used to determine changes in moisture content without using the dry density or mass attenuation coefficient of the soil. Unexplained variations in count rate occurred in the field. It was suggested that this problem was due to the temperature-sensitivity of the detector system. Magnesium and plexiglas bars were used as counting standards and accuracy was further improved by following established procedures, including frequent re-calibration. The system was capable of measuring moisture changes to within 1/2 inch of the soil surface.

Similar problems were encountered by Smith et al[42] who also concluded that definite instrument operating procedures were essential. The standard error of estimate reported for moisture determination in this study was $\pm$ 2.35 percent (volume basis).

A dual energy gamma ray transmission method for measurement of

water content and dry bulk density of soil was considered by Soane[44]. This system eliminated the need to measure water content and dry bulk density independently, allowing both of these properties to be measured concurrently in finite layers. The principle of the method was based on the variation of the ratio between the absorption coefficients for water and soil at different gamma energies. Experimental absorption coefficient ratios for sand and water were found to be $\mu_s/\mu_w = 1.6$ at 60 KeV and $\mu'_s/\mu'_w = 0.9$ at 660 KeV. The two gamma energies were supplied by ^{241}amerecium (60 KeV) and ^{137}cesium (660 KeV).

The variation in magnitude of the absorption coefficient ratio at different gamma energies permitted the solution of the following simultaneous equations for the values of mass thickness (g cm^{-2}) of soil (s) and water (w):

$$\ln I = \ln I_o - (\mu_s S + \mu_w W). \quad (2.5)$$

$$\ln I' = \ln I_o' - (\mu'_s S + \mu'_w W). \quad (2.6)$$

in which I and I_o are the primary energy count rates with and without the sample, and μ_s and μ_w are the mass absorption coefficients (cm^2 g^{-1}).

Although a detailed analysis of the experimental errors involved was not made, the results suggested that the double energy gamma transmission method may have considerable usefulness in soil tillage studies.

3. THEORY

3.1 Nature of Gamma Radiation

Atomic nuclei are presently believed to be composed of two major components: protons and neutrons[58]. The collective term for these is neucleons. Protons are positively charged particles, with a mass approximately 1850 times greater than that of an orbital electron. Neutrons are uncharged nucleons with masses approximating those of protons. The sum of the numbers of protons and neutrons in a given nucleus is the mass number.

The term isotopes refers to atoms that contain the same number of protons but varying numbers of neutrons and occupy the same place in the periodic table. In other words, they are atoms of the same atomic number, but differing mass numbers. An example is 14C which is an isotope of the element carbon with a mass number of 14. Since the symbol for the element implies the atomic number, the species is usually designated only by ^{14}C.

Although certain neutron-proton combinations in a given nucleus are possible, these isotopes may not be stable. Therefore, changes will take place resulting in an adjustment of the neutron to proton ratio so that the nucleus reaches a position of greater stability.

The nuclear changes referred to above involve spontaneous disintegration of one or more of the nucleons. Such disintegration results in the emission of particles and/or electromagnetic radiation from the nucleus. The electromagnetic radiation is in the characteristic form of discrete energy quanta known as gamma rays which are much like X rays, but considerably shorter in wavelength. Isotopes which emit

particulate or electromagnetic radiation are commonly termed radioisotopes.

Since radioactive decay involves the transformation of an unstable to a stable nuclide, it is an irreversible event for each atom. Unstable atoms of a given radioisotope do not all decay simultaneously. Instead, the decay of a given atom is an entirely random event and studies of radioactive decay events require the use of statistical methods. Decay rate is related to the degree of instability of a specific nuclide and is often expressed by the term half-life which is the time required for the activity of the nuclide to decrease by one half.

Radiation sources are commonly made up of solutions or compounds containing one or more radioisotopes. The strength or amount of activity of such sources is expressed by the standard unit of radioactivity - the curie. The term curie was defined arbitrarily in 1950[58] as 3.700×10^{10} disintegrations per second (dps). Subdivisions of the curie in common use are the millicurie (mCi) which is equal to 3.700×10^{7} dps and the micro curie (μCi) which is 3.700×10^{4} dps.

Gamma radiation, being made up of photons, does not carry electric charge nor significant mass, and consequently, can penetrate matter readily. Spectrum analysis of gamma rays reveals that they are emitted at defined energy levels which are measured in terms of electron volts (ev.). An electron volt is defined as the energy an electron would acquire while moving through a potential gradient of one volt.

The radioisotopes used in this experiment as gamma ray sources were cesium -137 (^{137}Cs) and amerecium -241 (^{241}Am) with peak gamma energies of 661 kev and 60 kev respectively.

3.2 Interaction of Gamma Radiation with Matter

The characteristic interaction of gamma radiation with matter provides a basis for measurement of moisture and density by the transmission method. Gamma rays interact with matter in at least six different ways, the most important of which are: photoelectric effect, compton effect and pair production.

Photoelectric absorption or scattering is the mechanism which accounts for much of the attenuation of electromagnetic radiation in the energy range of less than 0.1 Mev. A low energy photon interacts with an orbital electron of an atom and loses its entire energy in the ejection of the electron.

In Compton scattering, a photon collides with an electron and loses some of its energy. The lost energy is utilized in overcoming the binding energy of the electron and in accelerating the electron. The remaining photon energy results in a photon with lower frequency and longer wavelength. Compton scattering is the principal mechanism in the medium energy range (0.5 to 1.0 Mev).[58]

Pair production is a phenomenon occurring when a gamma ray interacts directly with a nuclear force field. In such an event, the photon ceases to exist and has all of its energy converted into two particles, a positron and electron. For this to take place, the incident gamma ray must have an energy equal to or greater than 1.02 Mev (the energy equivalent to the rest mass of one electron and one positron).

Compton effect and photoelectric effect are the primary modes of interaction involved in this experiment since the primary energies of ^{137}Cs and ^{241}Am are 0.661 Mev and 0.06 Mev respectively.

When a collimated beam of monoenergetic gamma rays passes

through an absorber, some of the energy of the beam is transferred to the absorber. For example, if an incident gamma beam of intensity Io passes through a thin absorber of thickness X, there will be a resulting decline in gamma intensity equal to ΔI. The resulting intensity of the emerging beam will be Io minus ΔI. Thus, the fraction of the beam intensity absorbed is proportional to the thickness of the absorber traversed or

$$-\frac{\Delta I}{Io} \propto x \quad \ldots\ldots\ldots\ldots\ldots\ldots\ldots\ldots\ldots (3.1)$$

The minus sign indicates that a decrease in intensity is occurring.

Introduction of a constant (the linear absorption coefficient of the material μ_l) which represents the fractional decrease in gamma intensity per unit thickness of the absorber, permits the conversion of this expression to an equation.

$$-\frac{\Delta I}{Io} = \mu_l \Delta x \quad \ldots\ldots\ldots\ldots\ldots\ldots\ldots\ldots (3.2)$$

Absorption is a continuous process throughout the thickness of the absorber. Therefore, the absorber's thickness may be visualized as a great number of infinitesimal thicknesses, (dx),and equation 3.2 can be integrated to give

$$\ln\frac{I}{Io} = -\mu_l x \quad \ldots\ldots\ldots\ldots\ldots\ldots\ldots\ldots (3.3)$$

where Io = incident gamma beam intensity

I = intensity of beam emerging from absorber

x = thickness of absorber.

The linear absorption coefficient (expressed as cm^{-1}) has the disadvantage that it varies considerably for different absorber materials. Since the absorption of gamma rays is primarily a function of the mass of the absorber[58], a more useful unit can be derived by taking the density

of the absorbing material into account.

Consider a volume of absorber that is one cm^2 in cross section and x cm long. The volume is numerically equal to the thickness (X) and the mass in this volume equals the density (P) times the thickness (PX). The fractional gamma absorption is proportional to the mass of absorber traversed and PX may be substituted in place of x in equation 3.1 to give

$$-\frac{\Delta I}{Io} \propto PX \quad \ldots\ldots\ldots\ldots\ldots\ldots (3.4)$$

The term mass absorption coefficient (μ) may now be introduced. It is the linear absorption coefficient (μ_l) divided by the density of the absorber or

$$\mu = \frac{\mu_l}{P} \quad \text{or} \quad \mu_l = \mu P \quad \ldots\ldots\ldots\ldots (3.5)$$

It follows that the units used will be $cm^2 g^{-1}$.

The mass absorption coefficient represents the fractional decrease in gamma intensity per unit of mass thickness (g cm^{-2}) of the absorber. Equation 3.3 can now be modified to give

$$\ln \frac{I}{Io} = -\mu PX \quad \ldots\ldots\ldots\ldots\ldots (3.6)$$

or

$$\ln \frac{I}{Io} = -\mu d. \quad \ldots\ldots\ldots\ldots\ldots (3.7)$$

where d is the mass thickness of absorber (g cm^{-2}).

3.3 Gamma-Ray Moisture and Density Detection

It is possible to determine the density or moisture content of a material based upon the absorption principle provided that only one of these properties varies. An early system, proposed by Vomocil[55], was based on the absorption of gamma rays as a logarithmic function of the wet bulk density. Laboratory studies of the single energy gamma

transmission method by Van Bavel et al[51], Van Bavel[50] and Reginato and Van Bavel[41] have shown that a high degree of sample resolution and accuracy can be achieved.

The theory of single energy transmission was explained by Reginato and Van Bavel[41] as summarized in the following three paragraphs.

For any compound or mixture of elements, the mass attenuation coefficient is

$$\mu = \mu_1 f_1 + \mu_2 f_2 + \ldots\ldots + \mu_n f_n \quad \ldots\ldots\ldots\ldots \quad (3.8)$$

where $\mu_{1\ldots n}$ = mass attenuation coefficients of the elements involved

$f_{1\ldots n}$ = the respective weight fractions of the elements.

The attenuation coefficient for a moist soil is

$$\mu = \left(\frac{\mu_s Ps + \mu_w Pw}{Ps + Pw}\right) \quad \ldots\ldots\ldots\ldots\ldots\ldots \quad (3.9)$$

where Ps = dry density (g cm^{-3})

Pw = volumetric water content (g cm^{-3})

The average value of attenuation coefficients of nine soils was $\mu_s = 0.0775\ cm^2 g^{-1}$. The value for water was given as $\mu_w = 0.0862\ cm^2 g^{-1}$.

In theory, there is no universally applicable value of μ for moist soils. However, values for μ_s and μ_w may be experimentally obtained using water and oven dry soil and the following relationship applies.

$$I = I_o e^{-(Ps\mu_s + Pw\mu_w)X} \quad \ldots\ldots\ldots\ldots\ldots \quad (3.10)$$

or

$$\ln \frac{I}{I_o} = -X\,(Ps\mu_s + Pw\mu_w) \quad \ldots\ldots\ldots\ldots \quad (3.11)$$

where I_o = unattenuated beam intensity

I = beam intensity after passage through the absorber

X = length of attenuation path.

Volumetric water content was calculated from the samples as follows

$$Pw = \frac{(\ln Io - \ln I - Ps\mu_s X)}{\mu_w X} \quad \ldots\ldots\ldots\ldots\ldots\ldots (3.12)$$

The dry density of the soil could be calculated similarly if the value of Pw was known for each sample. Neglecting the difference in attenuation coefficients between water and soil, water content could be calculated as follows

$$P'w = \frac{(\ln Io - \ln I)}{\mu_s X} - Ps \quad \ldots\ldots\ldots\ldots\ldots\ldots (3.13)$$

3.4 Principle of Dual Energy Transmission

Measurement of moisture content and dry bulk density using two gamma energies is based on variation of the ratio between the absorption coefficients for water and soil at different gamma energies. It was found by calculation[43] that the ratio between the absorption coefficients of soil and water depends markedly on photon energy below 100 Kev but only slightly at higher energies (figure 2). Certain practical aspects of this method have been investigated by Gardner and Fischer[18] and Soane[44] who independently selected ^{241}Am (60Kev) and ^{137}Cs (661Kev) as gamma sources to supply low and high photon energies respectively. Soane[44] found experimental absorption ratios, $\mu_s/\mu_w = 1.6$ and $\mu'_s/\mu'_w = 0.9$, for sand and water at low and high photon energies.

The variation in magnitude of the absorption coefficient ratio at different gamma energies permits the solution of two simultaneous equations

$$\ln I = \ln Io - (\mu_s Ps + \mu_w Pw)X. \quad \ldots\ldots\ldots\ldots\ldots (3.14)$$

$$\ln I' = \ln I'o - (\mu'_s Ps + \mu'_w Pw)X. \quad \ldots\ldots\ldots\ldots\ldots (3.15)$$

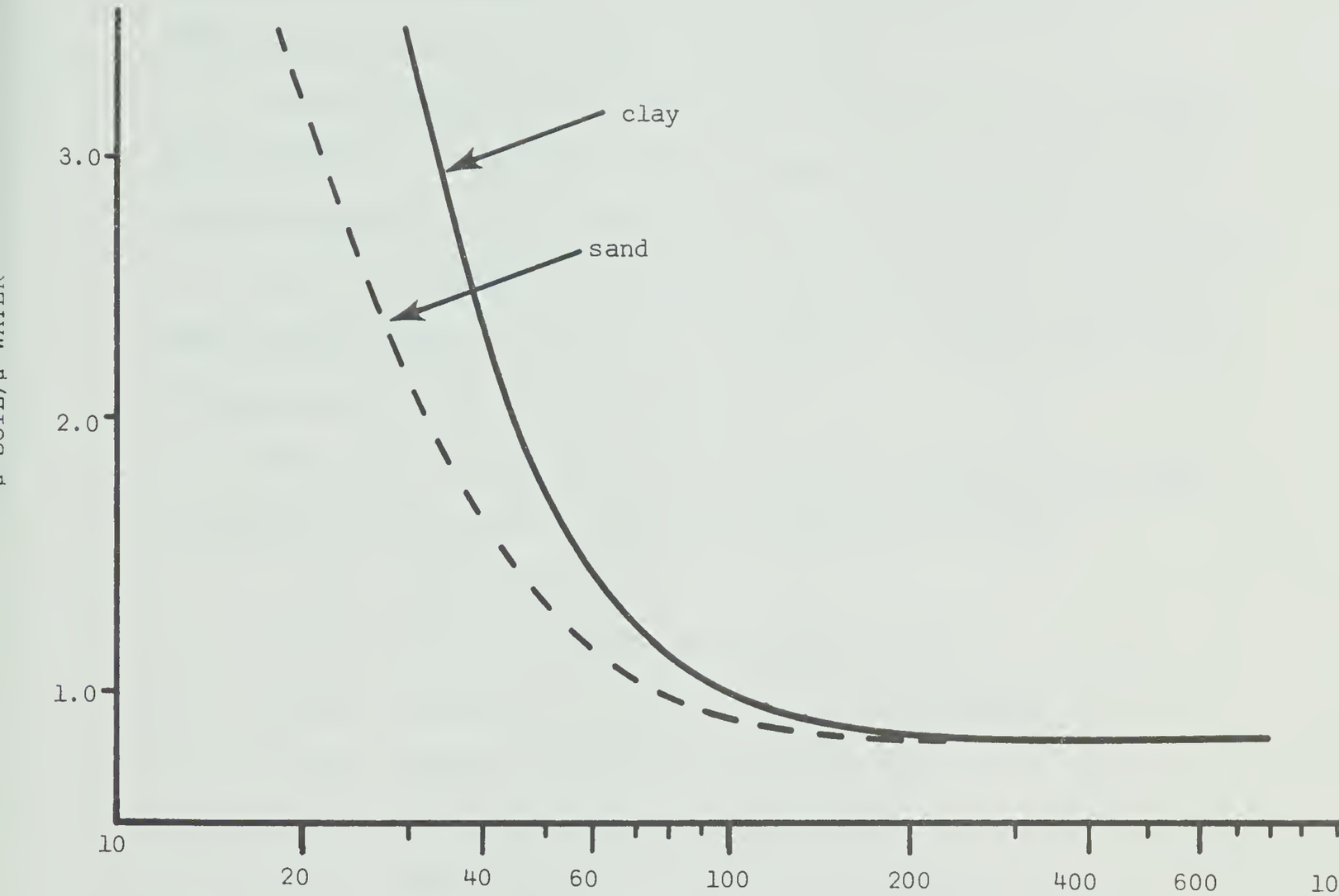

Figure 2: The relation between the ratios of absorption coefficients for soil and water and gamma ray energy for two contrasting soils (calculated)[43].

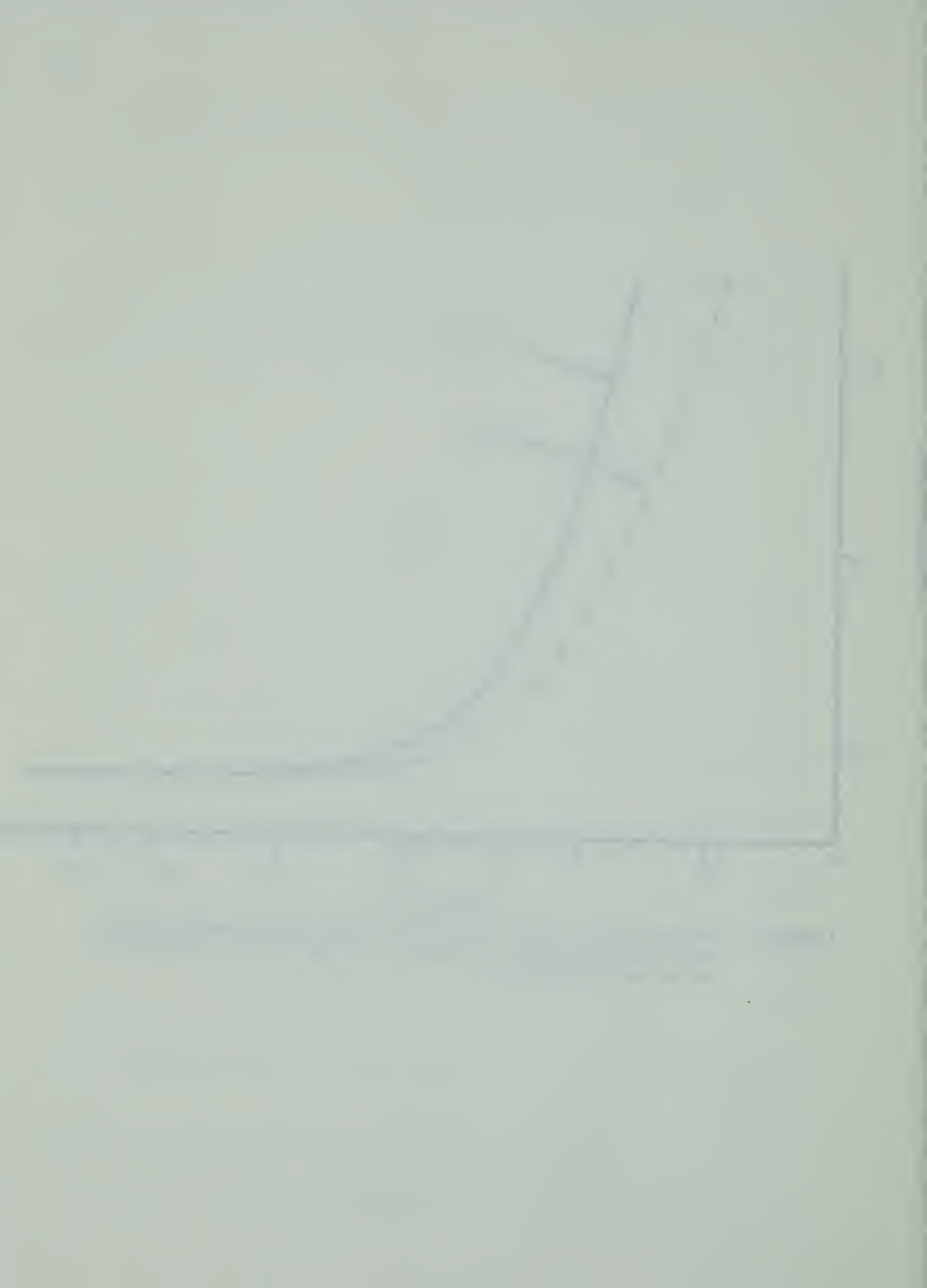

in which I and Io are count rates with and without the sample present, μ_s, μ_w, μ'_s and μ'_w are the experimental mass absorption coefficients ($cm^2 g^{-1}$) for soil and water at low and high energies, Ps and Pw are the dry bulk density (g cm^{-3}) and moisture content (g cm^{-3}) respectively and X is the sample thickness (cm).

For the purpose of this experiment, ^{241}Am and ^{137}Cs were used as gamma emitters. The choice of these isotopes was largely due to their availability and relatively long half lives (t 1/2 for ^{241}Am = 46o yr and t 1/2 for ^{137}Cs = 30 yr). In addition, both sources have well defined gamma energies which are sufficiently different to ensure a good degree of sensitivity of the method (figure 2).

The required strength for the two sources depends upon a number of factors associated with experimental conditions including:

i) sample thickness
ii) range of moisture and density expected
iii) separation distance of source and detector
iv) detector dimensions and efficiency
v) mode of electronic discrimination
vi) mass thickness of access tubes, source retainers and sample retainers
vii) degree of accuracy required.

Due to the low gamma energy emitted by ^{241}Am, two additional factors, self absorption and window absorption, must be considered. Self absorption refers to the amount of absorption by the radioactive compound itself and depends upon the mass thickness of the compound. Window absorpiton depends upon the mass thickness of the active face or "window" of the source capsule.

3.5. Scintillation Detection

Gamma rays may be detected (as a result of their interactions with matter) by gas ionization, scintillation and autoradiography. Scintillation detection is proportional and, when used with a pulse height analyzer, allows determination of the energy spectrum of the incident radiation. It is this factor which makes scintillation desirable over other types of detection for gamma transmission studies.

Scintillation detection is based on the interaction of radiation with substances known as fluors or scintillators. Excitation of the electrons in the fluor leads to emission of a flash of light (scintillation). The most common fluors used in gamma detection are thallium-activated sodium iodide crystals [NaI(Tl)][58].

Adjacent to the fluor in the detection assembly is a photomultiplier tube which converts photons or scintillations into electronic pulses. The magnitude of the output pulse from the photomultiplier is directly proportional to the quantity of energy dissipated by the incident gamma photon in the fluor. This factor makes it possible to electronically discriminate against all scattered or attenuated radiation and count only primary gamma photons. A total gain of up to 10^6 is produced by most photomultiplier tubes.

3.6. Radiation Protection

The control of radiation exposures of both radiation workers and the general public and the various aspects of radiological health have been examined in detail by Morgan and Turner[32] and Blatz[5]. Although much work has been done in this field, many of the biological effects of

radiation exposure are not well understood. Since there have been relatively few cases of accidental human overexposure, most radiation exposure standards have been based on theoretical considerations and the results of animal experiments. Geneticists generally believe, as a result of such experiments, that there is no threshold of radiation damage to genetic materials. That is, no matter how small the radiation dose, there will be some genetic damage in proportion to the amount of dose[5].

Recommended limits for radiation exposure have gone through a history of downward revision. Greater emphasis has been placed in recent years on the minimizing of all exposures to the lowest practicable values. The International Commission on Radiological Protection has set forth recommended exposure limits for radiation workers. Current exposure limits are as follows:

Maximum permissable dose (MPD), whole body:

5 rem /year

3 rem / quarter

100 mrem/ week

20 mrem/ day

The term rem (roentgen equivalent man) refers to the dose of any radiation which would have the same effect as one Roentgen of X or gamma radiation.

Two types of radiation monitoring were used during this experiment. First, all workers were provided with film badges by the Radiation Protection Division, Department of National Health and Welfare. Films were changed and developed at four-week intervals and radiation exposure reports returned to the users. The second type of monitoring

consisted of a portable survey meter or ionization chamber which was calibrated to read directly in mr hr^{-1}. This instrument was used when manipulation and handling of the sources was required.

An important factor affecting exposure from the sources used in this experiment is the inverse square law which states that radiation intensity varies inversely as the square of the distance. Therefore, an exposure rate of 100 mr hr^{-1} at one foot would be reduced to 100 x $1^2/2^2$ = 25 mr hr^{-1} at two feet.

To roughly determine the exposure from an external gamma-emitting source, the following empirical equation may be used[58]:

$$R = 6CE \quad . \quad (3.16)$$

where R = exposure rate in mr hr^{-1} at 1 foot

C = activity of source (millicuries)

E = total gamma energy per disintegration (mev)

Radiation exposure at one foot claculated by this method was R = 169.1 mr hr^{-1} for ^{137}Cs and 15.2 mr hr^{-1} for ^{241}Am. These values agreed fairly well with exposure rates of 145.0 mr hr^{-1}(^{137}Cs) and 15.5 mr hr^{-1} (^{245}Am) reported by the manufacturer of the sources.

4. INSTRUMENTATION

4.1 General Description of Moisture-Density Meter

The moisture-density meter consisted basically of two sections, a remote probe unit and a counting and control unit. The probe unit contained radioactive sources and a scintillation detector, both mounted on a remotely controlled positioning mechanism. The counting and control unit, connected to the probe unit by a fifty foot electrical cable, housed a pulse height analyzer, counter, timer and power supply. The schematic arrangement of these components is shown in figure 3.

4.2 Gamma Sources

Two gamma-emitting radioisotopes (^{241}Am and ^{137}Cs) were used as sources in the moisture-density probe. The complete source assemblies including source holder, capsule and shielding were supplied by Monsanto Research Corporation. Source specifications including activity and unshielded emission were supplied by the manufacturer (table 1). Each source was doubly encapsulated in welded stainless steel with two covers (each 0.005 inches in thickness) machined in place integral with the side walls. The double capsule was mounted with its active area on the center line of a stainless steel cylinder and held in place with a

TABLE 1: SOURCE SPECIFICATIONS

Isotope	^{241}Am	^{137}Cs
Energy (kev)	60	660
Activity (mCi)	422	42.65
Emission (mr hr^{-1})	15.5	145.0
Half life (yr)	458	30

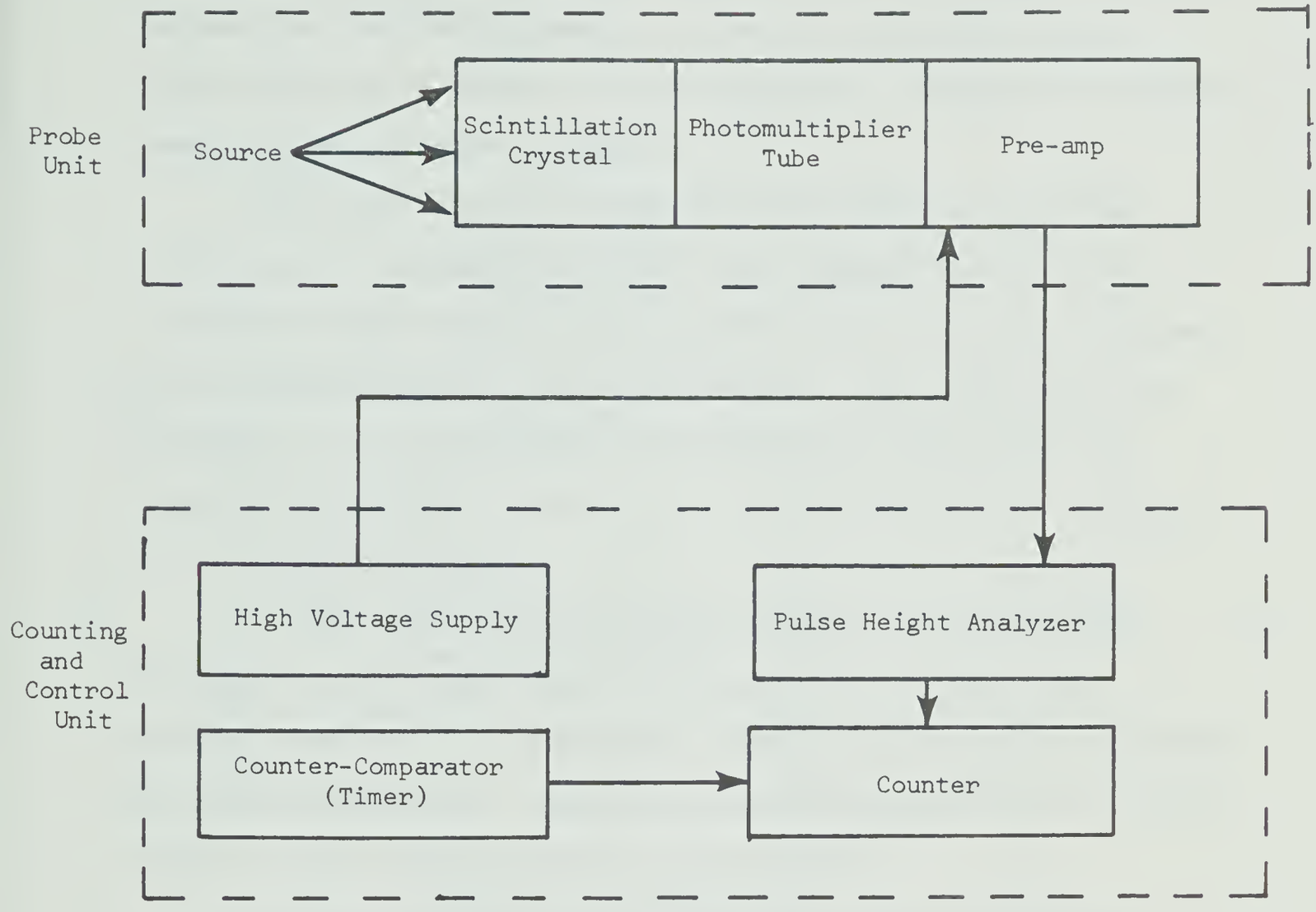

Figure 3: Schematic arrangement of counting and detection system.

retaining bushing. A threaded plug was used to press the source capsule against the retaining bushing. Shielding of the source was achieved by enclosing it in a six inch O.D. brass cylinder. The source could be lowered from the shield by means of a 3/4 inch rod equipped with a safety wedge key to prevent accidental exposure. A diagram of a complete source assembly is shown in figure 4.

Due to the relatively low gamma energy emitted by the ^{241}Am source, and the configuration of the source capsule, the effective activity was significantly reduced by the window of the source container and by self absorption in the source material itself. The count rate obtained was low in comparison to the count rate obtained from the higher energy caesium source.

4.3 Detection Equipment

Gamma detection was achieved by using a modified Nuclear-Chicago DS-202 well-type scintillation detector. Basically, the detector consisted of a scintillation crystal, a high gain photomultiplier tube and a preamplifier. Output pulse from the preamplifier was positive with 0.25 μ sec rise time and 70 μ sec decay time.

The well-type detector was designed primarily for counting samples prepared in a test tube or small bottle and placed in the well of the scintillation crystal. Three modifications were necessary to accommodate the external sources and geometry used in this experiment.

The first modification consisted of replacing the well-type scintillation crystal with a solid two inch by two inch sodium iodide, thallium activated [NaI (Tl)] crystal. Since the incident radiation beam was at a right angle to the detector axis, the original crystal retaining assembly was replaced by a lead shield and retainer with a

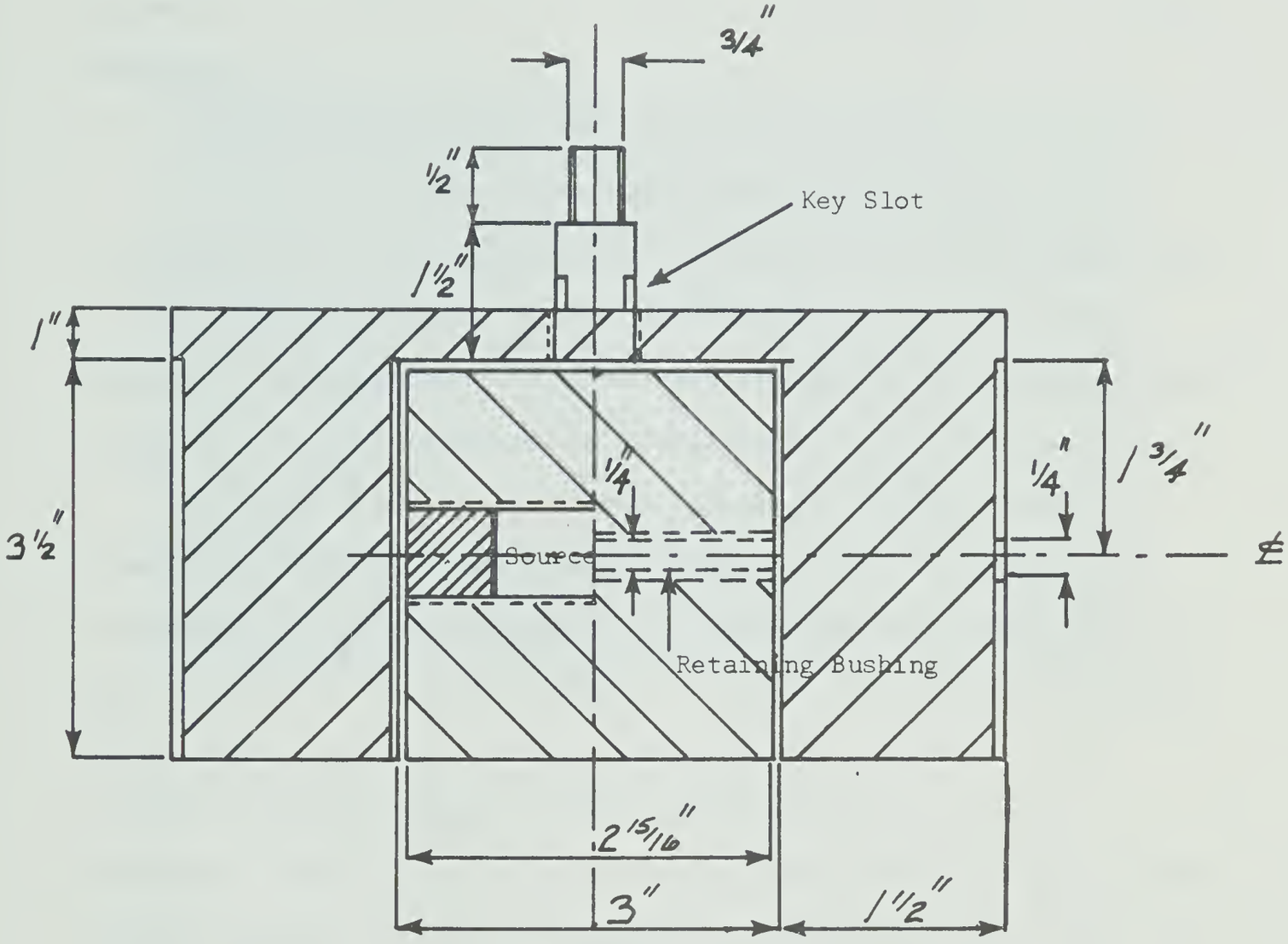

Figure 4: Source assembly.

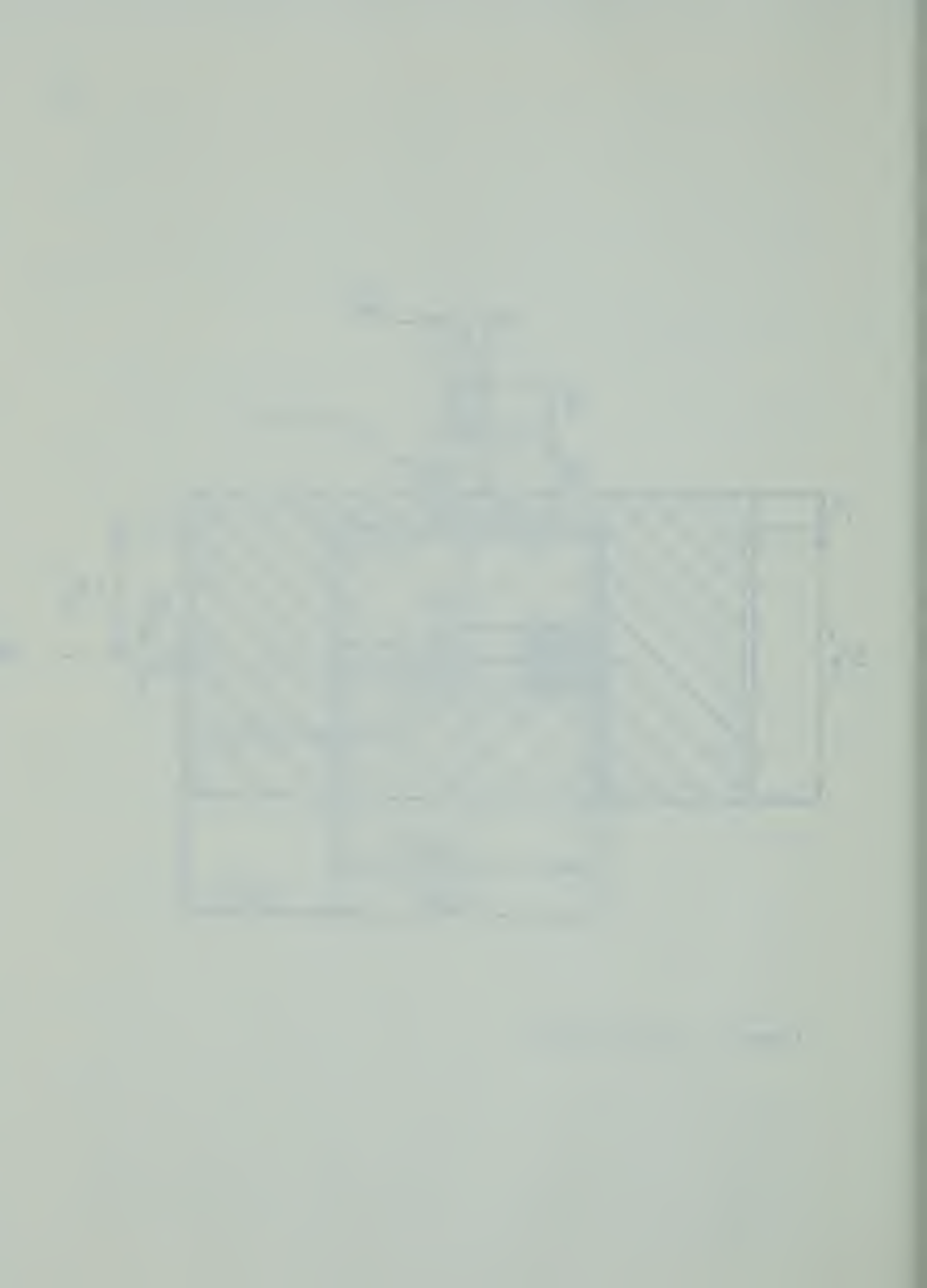

1 1/2 x 1 1/2 inch side window. This was the largest window possible with the given detection system and was necessary due to the relatively low count rate obtained from the americium source. The third modification consisted of attaching the detector to the probe mechanism by means of a 3/4 inch rod. The modified detector assembly is shown in figure 5.

4.4 Differential Discriminator

A differential discriminator (pulse height analyzer) was incorporated into the counting system to exclude all pulses except those of the primary photopeak. Pulses resulting from electronic noise, background radiation and scattered radiation were rejected and increased counting efficiency (maximum sample-to-background ratio)[58] was achieved.

To serve the purposes of this experiment, without incurring unnecessary expense, a pulse height analyzer (pha) was designed and constructed to function within the required range of count rates. The pha consisted of two discriminators or "gates" which passed only those pulses whose heights lay between their settings (figure 6). The "window" (channel) height and width were adjustable so that the instrument could be used to determine the entire energy spectrum of the incident radiation or set to straddle the primary photopeak (figure 7).

The basic components used in the pulse height analyzer circuit consisted of four solid state differential input amplifiers driven by a fifteen volt DC regulated power supply. The amplifiers were specified by the manufacturer as having ~ 500,000 V/V dc gain, rated output of $\pm$ 10v and full output frequency of 100kHz. A circuit diagram of the pha is shown in figure 8.

Figure 5: Modified scintillation detector.

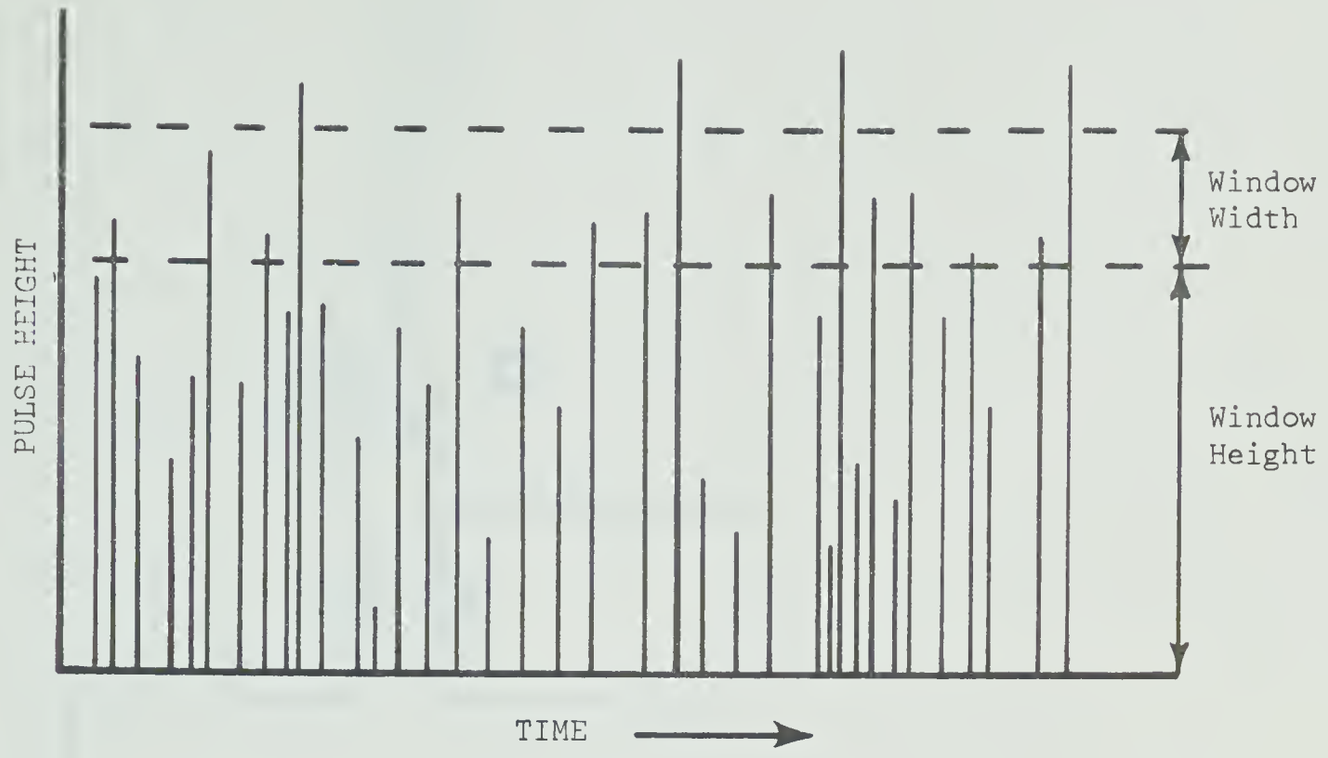

Figure 6: Operation of a pulse height analyser.

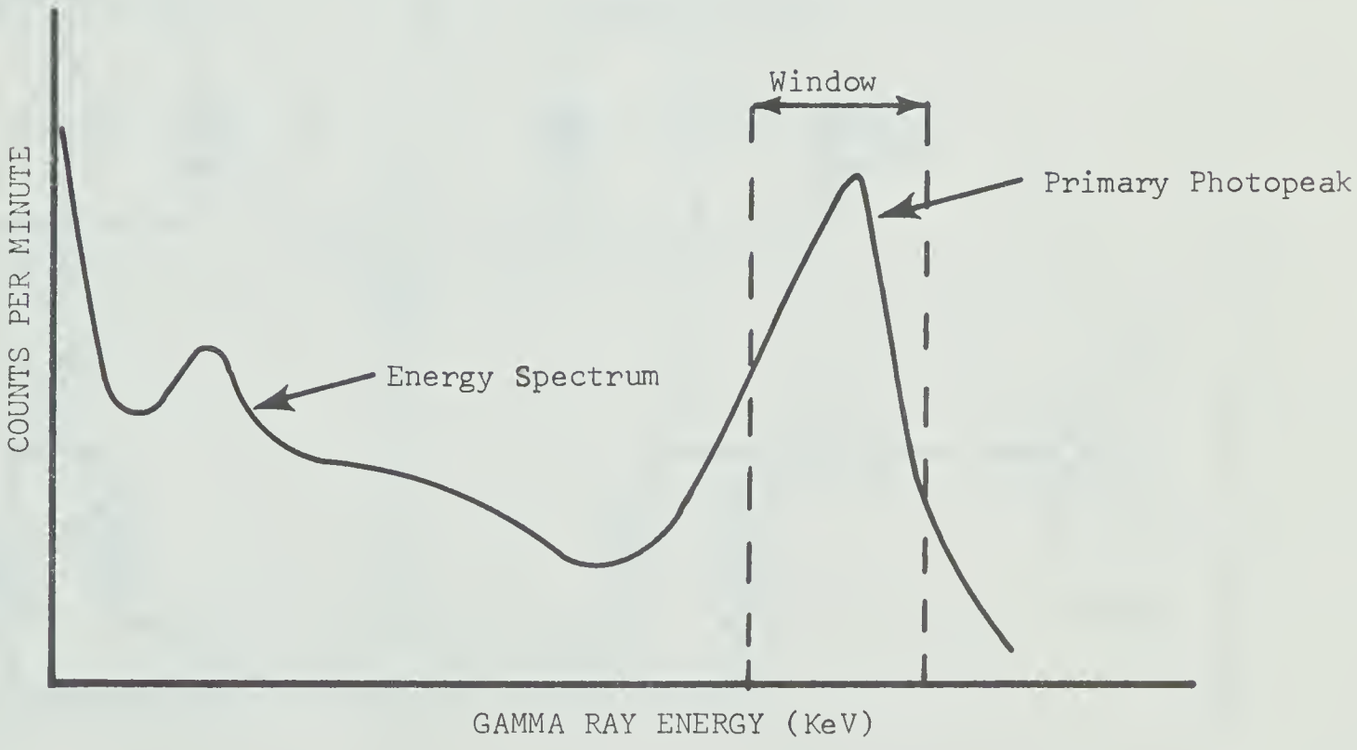

Figure 7: Typical gamma energy spectrum showing pha window straddling primary photopeak.

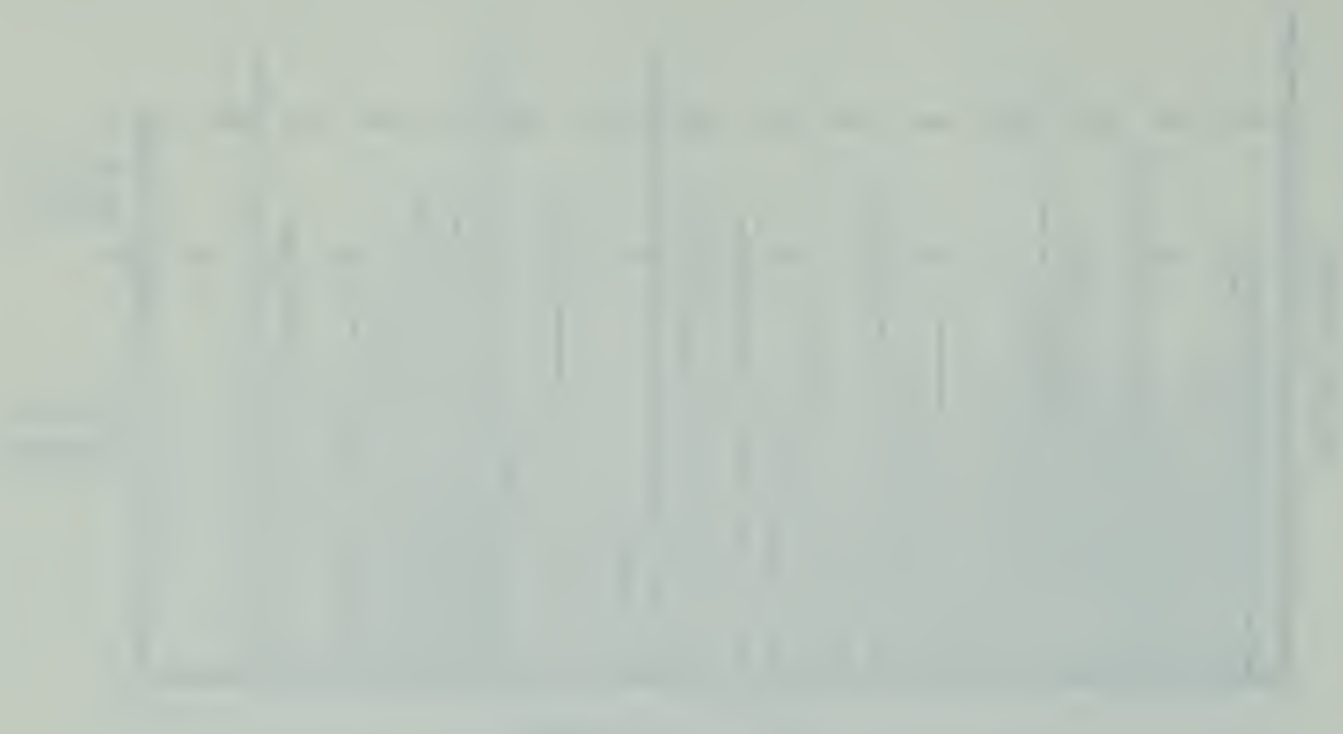

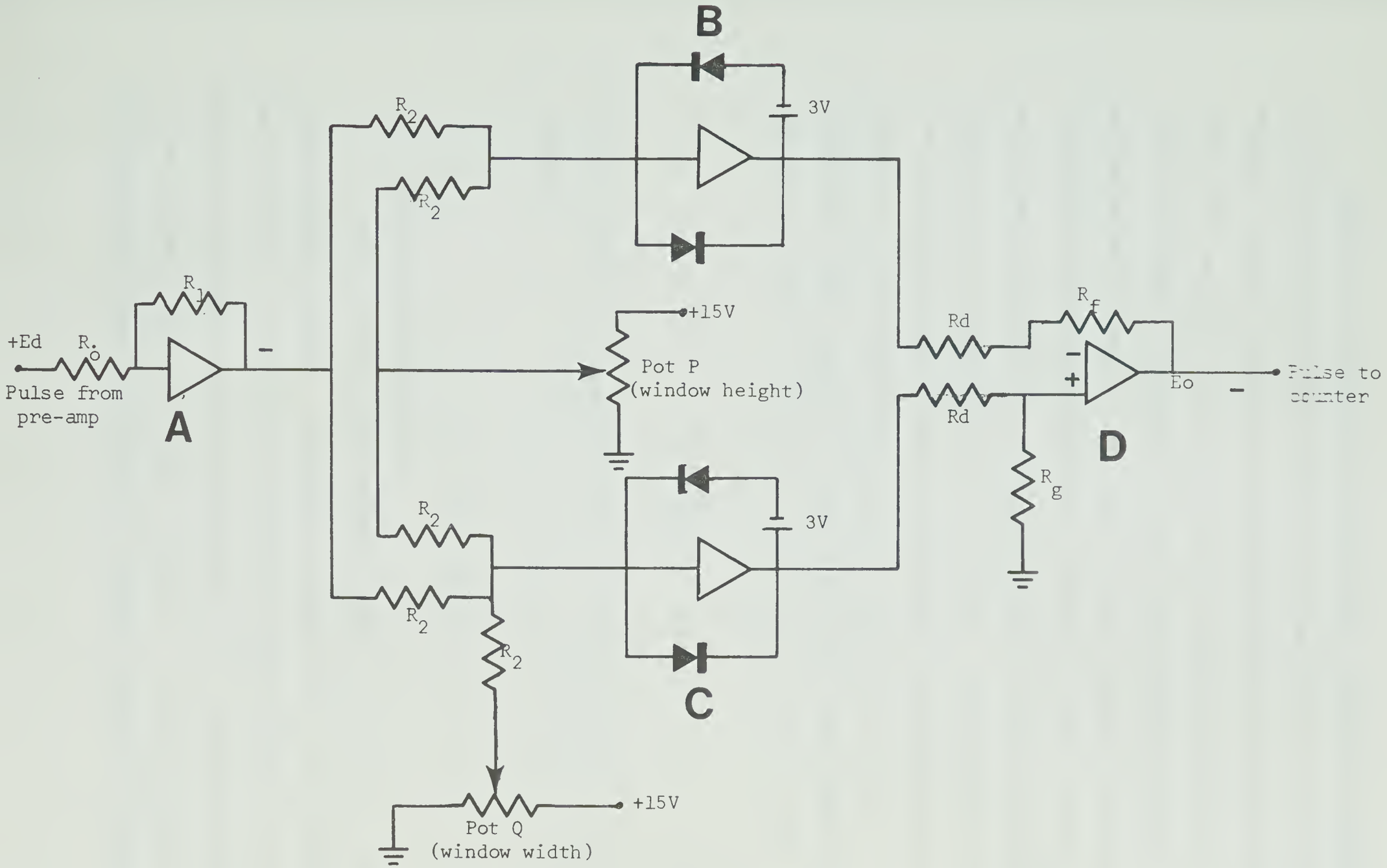

Figure 8: Pulse height analyzer circuit.

Amplifier A was used as a variable gain inverter to amplify the output pulses (Ed) from the detector preamplifier. The changing of resistor R_1 made it possible to attain approximately the same voltage output from amplifier A for both the 60 kev americium and 660 kev cesium photopeaks. Amplifiers B and C were essentially function generators which served as the upper and lower levels of the pha window. Each amplifier was output bounded by a feedback network consisting of two diodes in series with a floating voltage, the series combination being such as to bound the output at +3 volts. Window height and width were determined by potentiometers P and Q which controlled bias voltage supplies to function generators B and C. The function of the differential input amplifier, D, was to pass only those signals resulting from pulses which fell within the window of the analyzer so that

$$E_o \simeq \frac{Rf}{Rd}(E_2 - E_1) \quad . \quad . \quad . \quad . \quad . \quad . \quad . \quad . \quad . \quad (4.1)$$

Since the circuit was designed so that Rf = Rd, equation 4.1 may be written as

$$E_o \simeq (E_2 - E_1) \quad . \quad . \quad . \quad . \quad . \quad . \quad . \quad . \quad . \quad . \quad . \quad (4.2)$$

4.5 Counting and Timing Units

Pulses from the pulse height analyzer were fed into a Beckman 7050 electronic counter. The maximum counting rate of the instrument was specified as 100 Kcs and its registered count capacity was 100,000. The mode of operation used was designated as C/B - A with the components of the counter connected as shown in figure 9. In this operating mode, the instrument counted pulses input to channel C during the interval

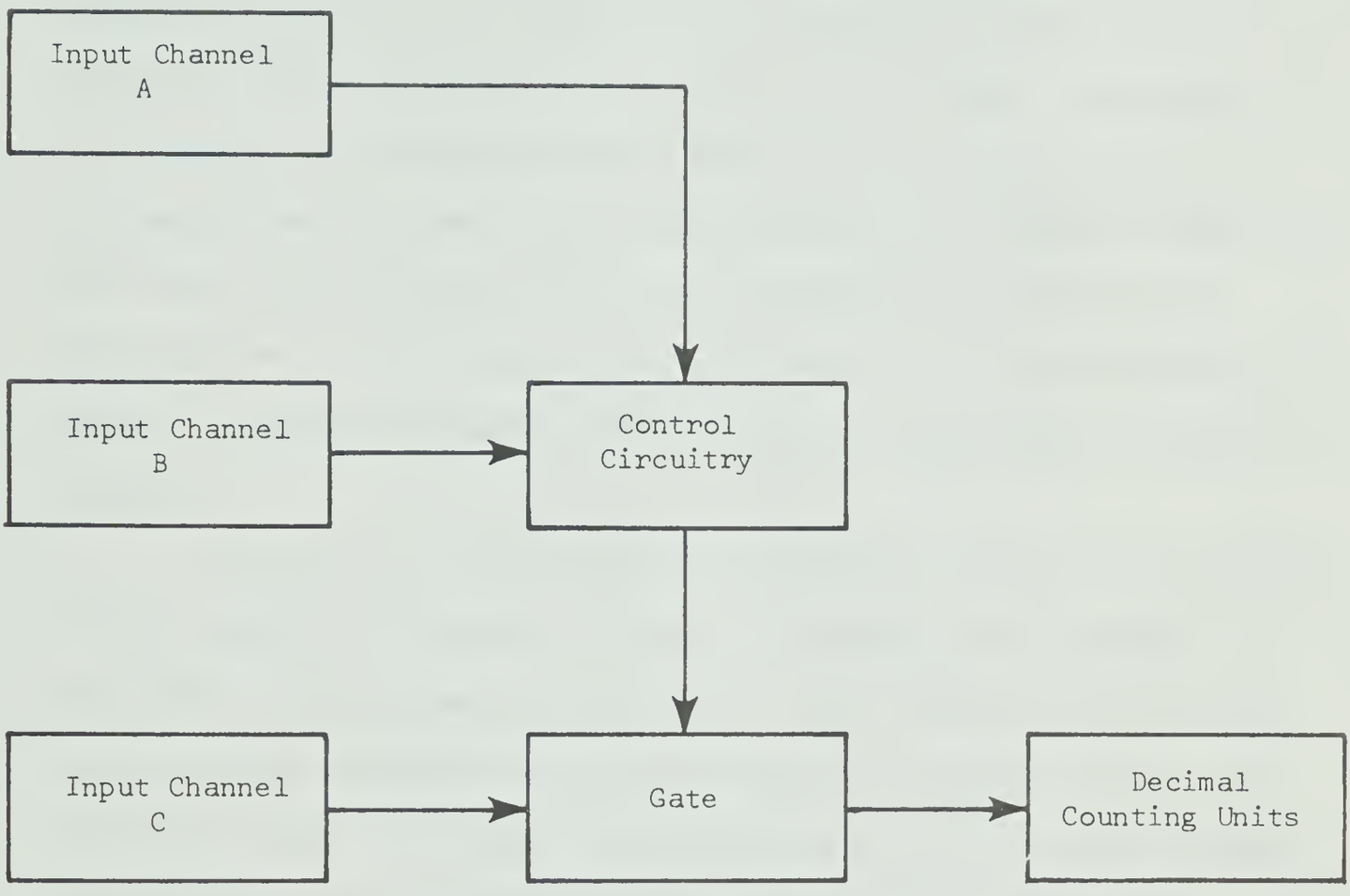

Figure 9: Electronic counter in C/B-A mode.

separating start and stop pulses input to channels B and A respectively.

Timing of the counting interval was accomplished by using a second electronic counter in conjunction with a digital comparator. The second counter was also operated in the C/B - A mode and a line frequency signal (60 Hz) was fed into the C input channel. The function of the digital comparator was to compare an input number (in this case, line frequency count) bit by bit with a pre-set limit number. For example, a limit number of 3600 representing a time period of one minute was used throughout the experiment. The time required for one complete comparison was about 10 milliseconds and a visual and electrical indication was provided when the input number was below, equal to, or above the limit number. A schematic diagram of the counter and timer system is shown in figure 10.

A pulse from the start switch, S, initiated counting simultaneously in both electronic counters, with one unit counting line frequency and the other counting pulses from the pha. A limit number of 3600 was set on the digital comparator and when this number was reached by the line frequency counter, the comparator provided an electronic pulse which was fed back to channel A of both counters. Counting was terminated simultaneously in both counters after a period of one minute. Radiation intensity in counts per minute could then be read directly from the radiation counter. The electronic counters and the digital comparator are shown in figure 11.

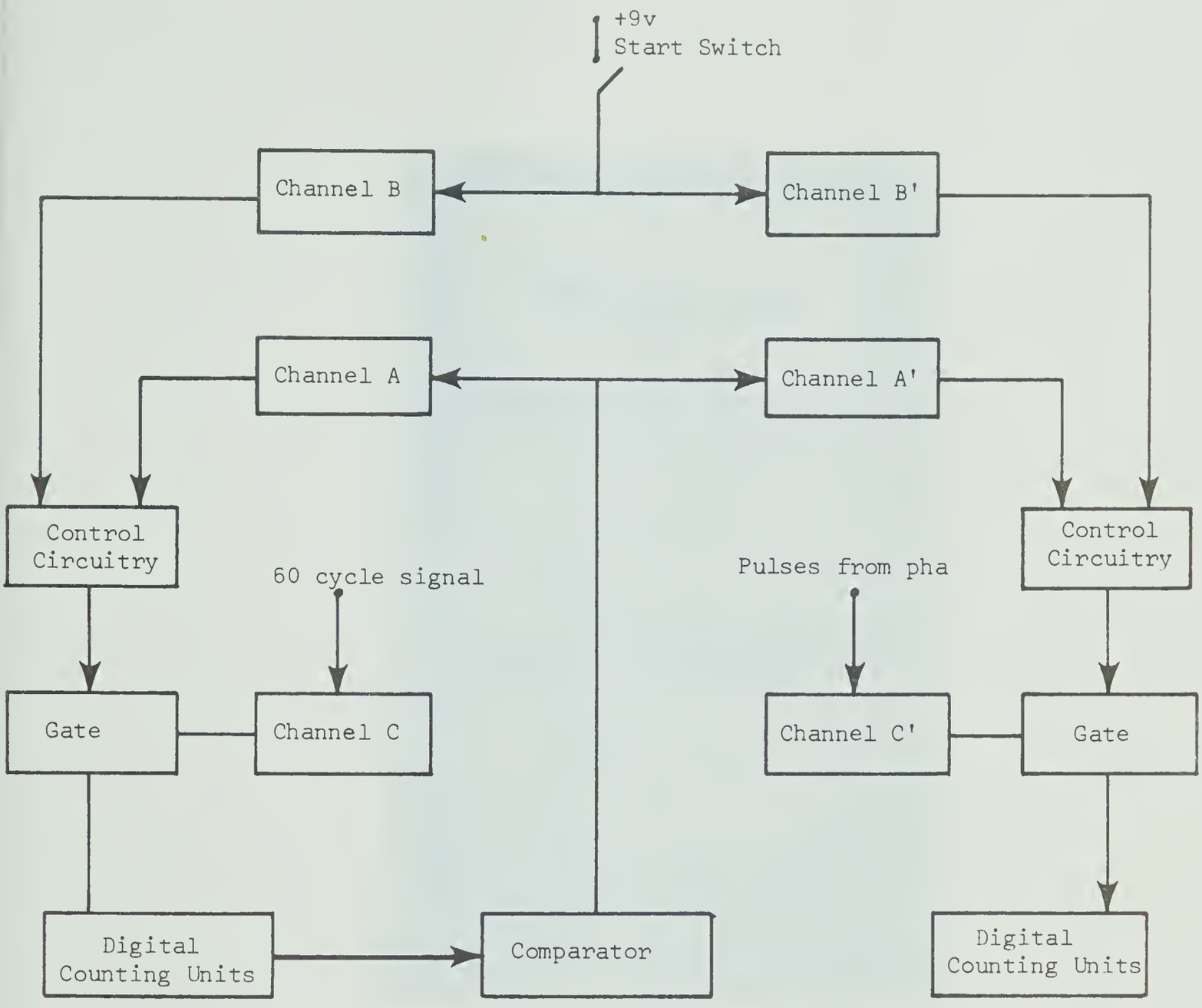

Figure 10: Counting and timing system.

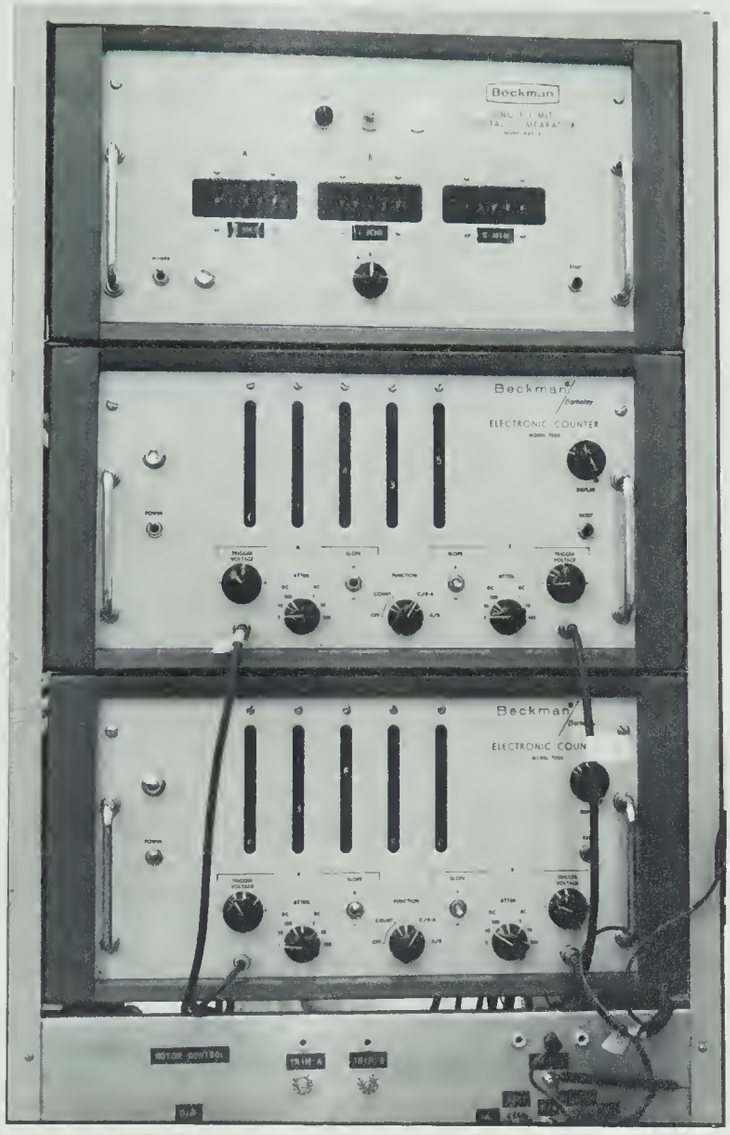

Figure 11: Electronic counters and digital comparator.

4.6 Probe Apparatus and Controls

The primary purpose of the probe unit was to enable the position of the source and detector to be remotely controlled so that moisture and density readings could be obtained with minimum exposure of the operator to gamma radiation. The lifting mechanism for the source and detector (figure 12) consisted of two mandrel assemblies (A), each consisting of a sprocket with a mounted bronze hub (B) which was threaded to accommodate a 3/4 inch lifting rod (C). A twelve volt, series wound, AC-DC motor was used to drive the mandrels. Counter weights (D) were installed to compensate for the weight of the source and detector and thereby lengthen the life of the bronze bushings. The sources were attached to the lifting rod by means of flange E. The upper half of this flange was spot-welded to the lifting rod to ensure that the axial position of the sources remained unchanged throughout the experiment. Accurate positioning of the source and detector was necessary before each reading was taken. Therefore, four micro switches (figure 13), each spaced four inches apart, were mounted on an adjustable bracket (A). The switches were operated by a flag (B) mounted on the source lifting rod. As the source and detector proceeded downward, the flag contacted the first micro switch which opened the circuit and stopped the drive motor. The source and detector remained in this position until a push-button "over-ride" switch (mounted on the control panel) was used to by-pass the first micro switch, allowing the assembly to proceed down to the second micro switch. This control system was primarily designed for use in field studies where measurements were to be taken at four-inch intervals. However, it also proved useful in the laboratory experiment as a method of positioning the source and detector

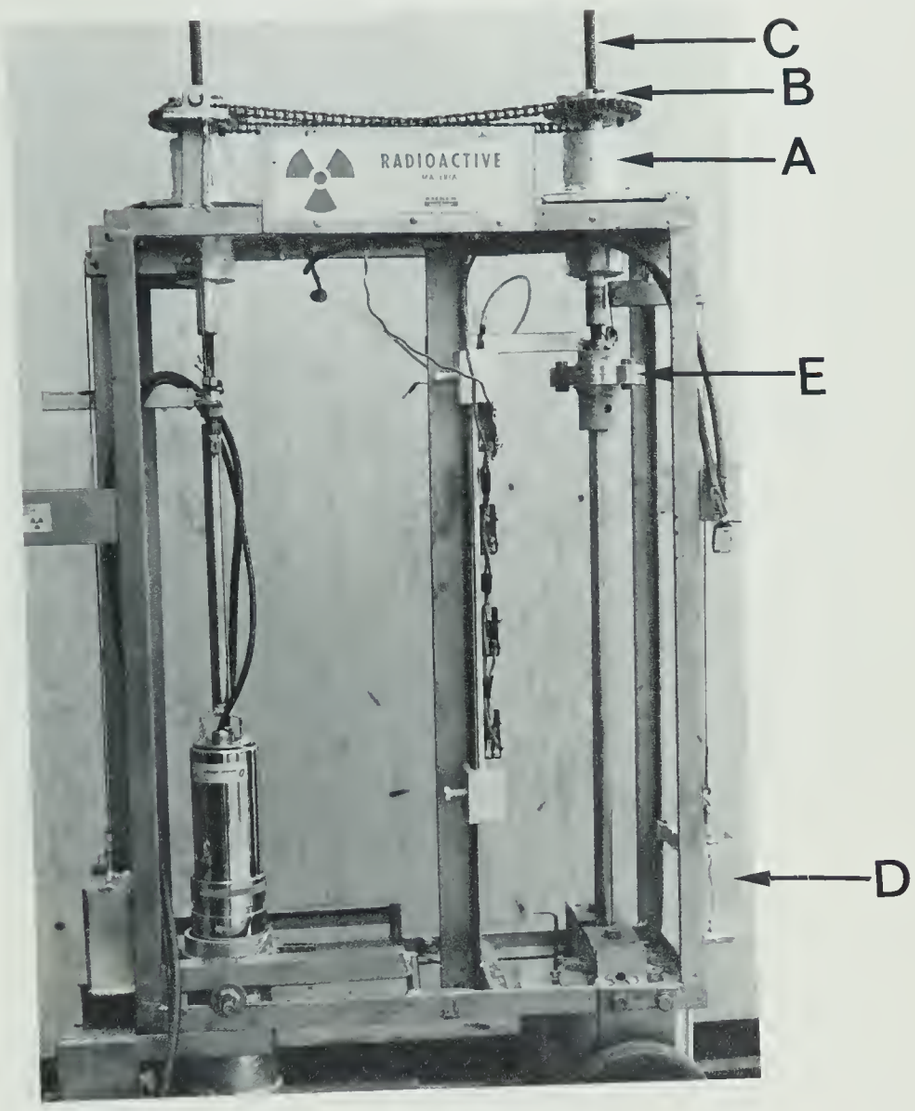

Figure 12: Lifting mechanism.

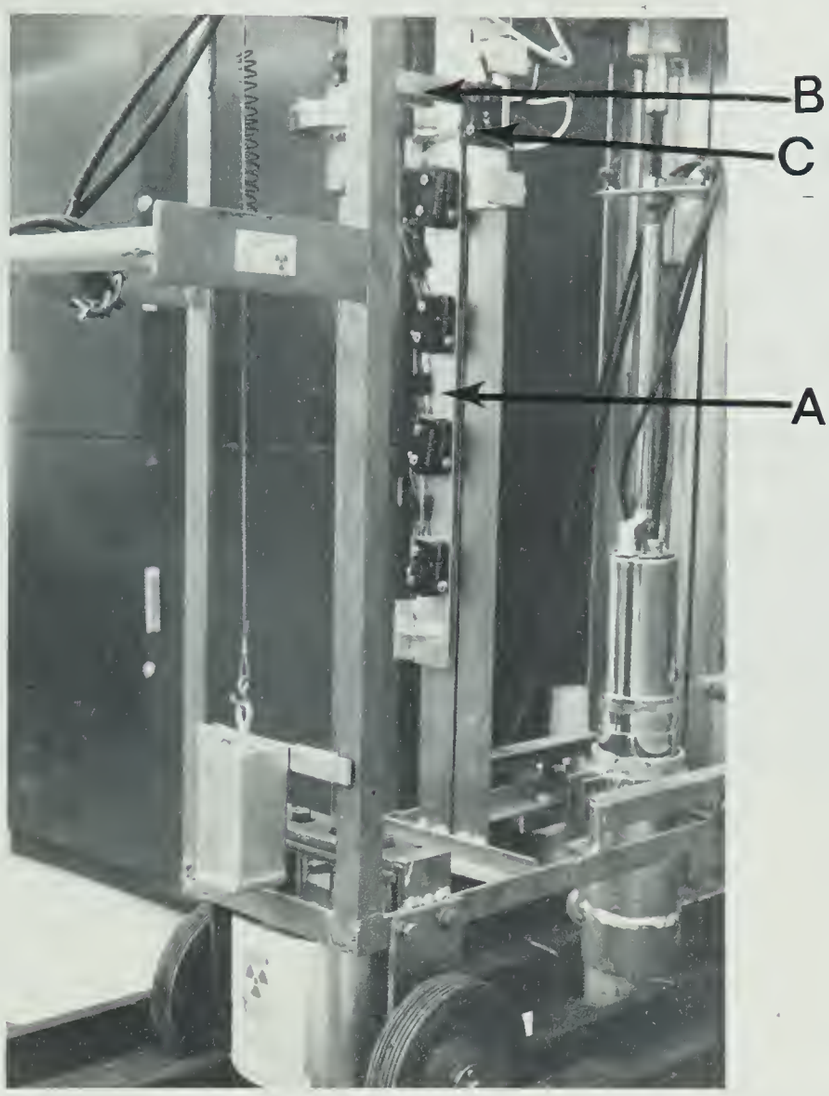

Figure 13: Micro switches.

in relation to the samples. An upper limit micro switch (C) was also installed to stop the motor when the probe assemblies had reached the end of their upward travel.

On-off, up-down, and over-ride functions were all controlled by switches mounted on the counting and control unit.

4.7 Radiation Protection Equipment

Radiation monitoring was required to determine whether workers were receiving radiation exposures within the generally accepted maximum permissible doses. Atomic Energy Control Board regulations required the wearing of monitoring films by all personnel working with the sources. As an additional precaution, a portable survey meter (ion chamber) was used when handling of the sources was necessary. This instrument provided quick rate-of-dose measurements in mr hr^{-1}.

A film badge and the survey meter are shown in figure 14.

Figure 14: Film badge and survey meter.

5. PROCEDURES

5.1 Calibration

The equipment used in this experiment was constructed from a number of components, some of which were built or modified locally to perform a specific function. Detailed calibration procedures were necessary to assure satisfactory performance of the system as a whole.

5.1.1 Optimum Gain versus High Voltage

Pulses counted by the scintillation detection system were the result of two factors, viz. the gamma source and background. Background pulses, arising from background radiation, thermal noise in the photo-multiplier and electronic noise, were undesirable. This made it necessary to minimize the contribution of background to the total counting rate so that the ratio of the square of the sample count rate to the total background count rate was at a maximum (S^2/B = max.)[58].

The determination of optimal operating conditions for the detection system involved two parameters; the potential applied to the photomultiplier and the gain of the pulse height analyzer amplifier. An increase in potential to the photomultiplier improved detection efficiency but also increased background counting rate. Increases in amplifier gain increased the sample counting rate but contributed relatively little to background.

At a fixed gain setting, a series of activity determinations were made at successively higher photomultiplier potentials. The source was removed and background counts were taken at the same settings. Amplifier gain was then increased and the process repeated.

For the cesium source, the ratio S^2/B was at a maximum when

photomultiplier potential was at 1050 volts and the amplifier gain was 25. The same process was repeated for the amerecium source and optimum operating conditions were found to be 1100 volts photomultiplier potential with an amplifier gain of 250.

5.1.2 Spectrum Calibration

In order to determine the location of the primary photopeaks, the actual line spectrum was found for each gamma source. This was accomplished by placing a suitable absorber (in this case a 0.75 inch lead plate) between the source and detector to reduce the radiation intensity to a level which could be handled by the counting equipment. The window width of the pha was set at 0.1 volts with the base of the window at 0 volts. Count rates (cpm) were taken as the window height was increased in 0.1 volt increments. Continuous gamma ray spectra were obtained for the amerecium and cesium sources and are shown in figure 15. This figure shows that the 60 kev photo peak for amerecium occurred at a pha setting of 6.7 volts while the 660 kev cesium peak occurred at 6.0 volts. By using these gamma spectra as a basis, it was possible to set the pha window to straddle the primary photopeak of each gamma source. Background amounted to 1,448 cpm at the amerecium setting and 250 cpm at the cesium setting.

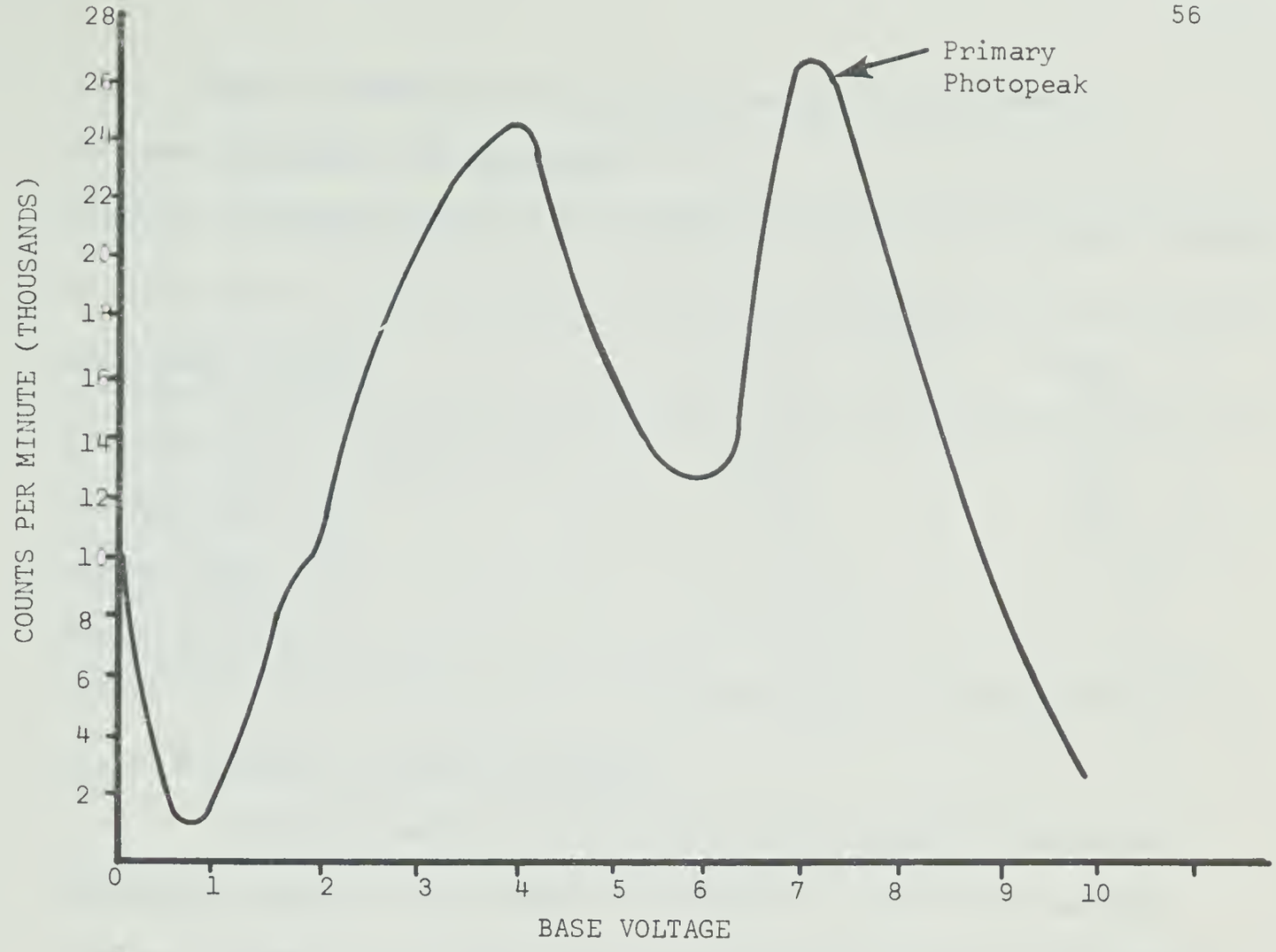

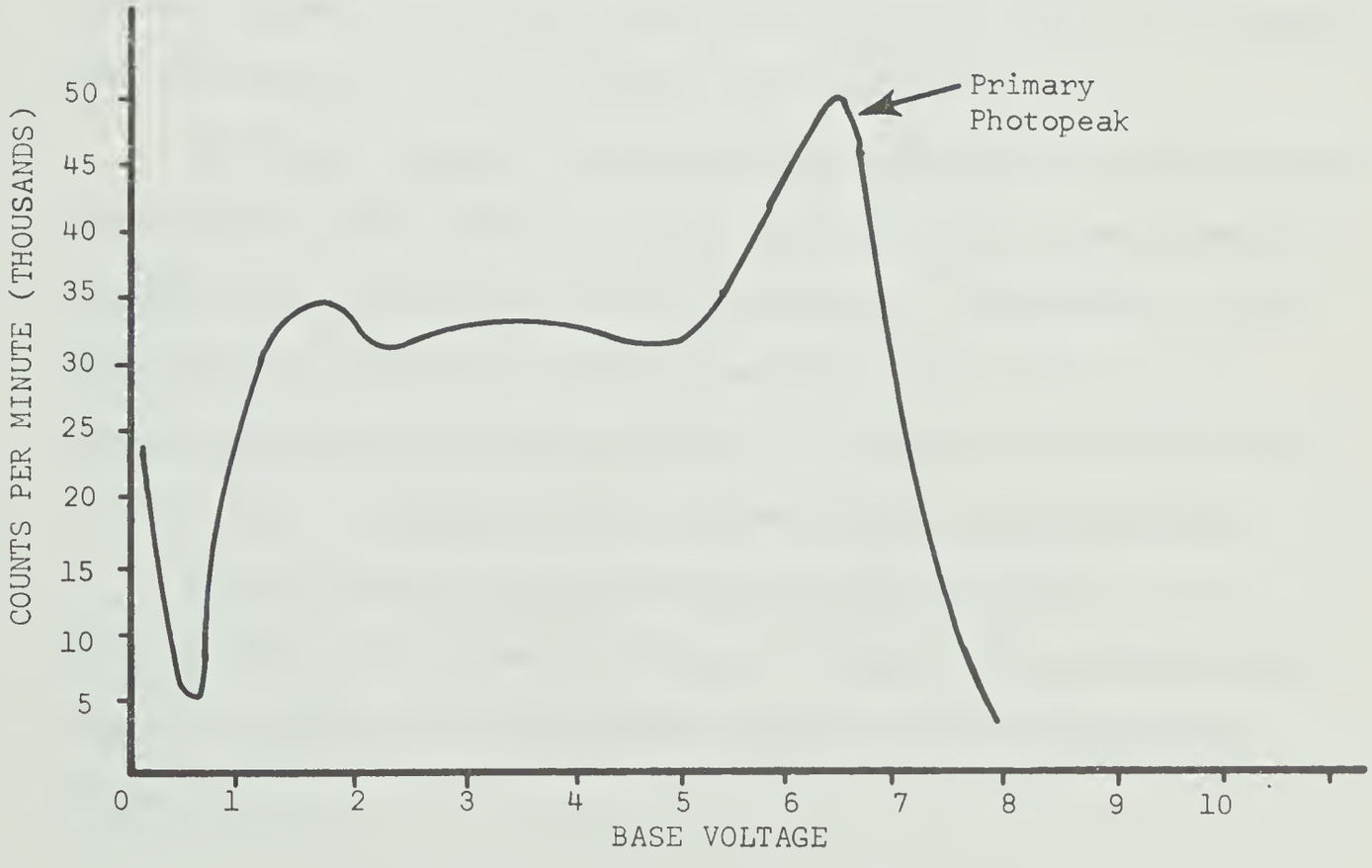

Figure 15: Gamma ray spectra for amerecium^{-241} (top) and cesium^{-137} (bottom).

Table 2 summarizes the instrument settings established and followed throughout the experiment.

TABLE 2: INSTRUMENT SETTINGS ESTABLISHED FOR AMERECIUM AND CESIUM SOURCES

Instrument Setting	Source ^{137}Cs	Source ^{241}Am
Photomultiplier Potential (V)	1050	1100
Pha Amplifier Gain	25	250
Window Height (V)	5.0	5.9
Window Width (V)	1.5	1.5

5.1.3 Horizontal and Axial Alignment

A limited amount of collimation was provided by the source containers (section 4.3), making it desirable to achieve and maintain precise alignment of the gamma beam with the active face of the detector. Both horizontal and axial alignment were considered.

Horizontal alignment was achieved by removing the drive chain on the probe unit and raising the source probe so that the gamma beam was slightly above the active face of the detector. The position of the gamma beam was monitored by taking one-minute counts with the pha window straddling the primary photopeak. The source probe was lowered in 0.125 inch increments until a maximum count rate was obtained.

Axial alignment involved rotating the source probe on its vertical axis until maximum counts were obtained. The probe was locked in place by means of two set screws located in the mounting flange (figure 12, E).

5.1.4 Counting Standards

The detection system was extremely sensitive to changes in photomultiplier potential (drift in high voltage supply). Temperature changes were also found to affect the counting rate.

To overcome this difficulty, counting standards of constant mass thickness were used. A 0.25 inch copper sheet was used for the low energy amerecium source. This sheet was placed between the source and detector and a series of ten one-minute counts were taken. The mean net counting rate was 78,346 cpm with a standard deviation of 408 cpm. Throughout the remainder of the experiment, a one-minute count was taken through the copper standard immediately preceeding each sample count. The ratio of this count to the mean value of the standard count was used as a correction factor for the sample count rate so that

$$\text{corrected sample (cpm)} = \frac{\text{standard (cpm)}}{\text{mean standard (cpm)}} \times \text{sample (cpm)}$$

The higher energy of the cesium source made it possible to use the 1.5 inch brass shielding of the source container as a counting standard. The mean count rate for this standard was 277,932 cpm with a standard deviation of 2,809 cpm.

5.1.5 Preparation of Calibration Samples

Mass attenuation coefficients for water (μw) and soil (μs) were required for both gamma sources. Samples of oven-dry soil and water of varying mass thicknesses were prepared. The calibration samples were prepared in a five-inch I.D., thin walled steel tube with a rigid plastic cover at one end. The cross-sectional area of the tube was 119.6 cm^2. Oven-dried soil was placed in the tube and held in place with a snug-

fitting one inch styrofoam plug during the measuring period.

Water samples were accommodated by placing a polythene bag in the sample tube. The bag was filled to the required level, sealed, and held in place with a styrofoam plug.

5.1.6 Determination of Calibration Curves

Values for μs and μw were obtained by plotting calibration curves for soil and water for each gamma source. Each curve was obtained by plotting the log of the sample count rate (cpm) versus absorber mass thickness (g cm^{-2}). The mass absorption coefficient for each combination of source and absorber was equal to the slope of the curve. Four calibration curves were required and are shown in Appendix I together with the raw count rate data. Two count rates were taken at each mass thickness and averaged to minimize sampling error.

Absorber mass thickness (g cm^{-2}) was determined by weighing the amount of absorber (soil or water) placed in the sample tube and dividing by the cross-sectional area of the tube. Physical limitations of the probe unit and counting system prevented a wider range of mass thicknesses from being used. Calibration samples were measured with the same geometry and counting techniques used throughout the experiment.

Mass absorption coefficients obtained from the calibration curves by non-linear regression techniques[58] are summarized in table 3. Values of un-attenuated count rates (I_o and I'_o) were obtained by extrapolating the calibration curves for each source to zero mass thickness. These values were:

$$I_o = 909,910 \text{ cpm (Cesium)}$$

$$I'_o = 17,980,000 \text{ cpm (Amerecium)}$$

TABLE 3: MASS ABSORPTION COEFFICIENTS FOR SOIL AND WATER AT TWO GAMMA ENERGIES.

Absorber	Source ^{137}Cs	Source ^{241}Am
Soil	$\mu s = 0.0646$	$\mu' s = 0.2724$
Water	$\mu w = 0.0690$	$\mu' w = 0.1925$

5.2 Experimental Procedure

The experiment was carried out at the Agricultural Engineering research facility at Ellerslie, Alberta. Soil samples, obtained from a nearby plot were moisturized and compacted in the laboratory. After initial moisture and density measurements were made, the samples were placed in a walk-in freezer unit at the Animal Science Farm, Edmonton, where the freezing portion of the experiment was carried out.

5.2.1 Experimental Design

The variable studeid was density change, D. The factors studied which may influence density change were:

Factor	Code	Levels
Freezing Temperature	A	$+10^{\circ}$, -5°, -20°, F
Moisture Content	B	15%, 25%, 35%
Initial Density	C	60 pcf, 70 pcf, 80 pcf

Freezing temperatures could not be randomized over an entire replicate because only one freezing compartment was available. Therefore, a split plot design was used with each of the independent variables at three levels. The experiment was replicated three times. A complete mathematical description for any observation is:

$$Y_{ijkl} = \mu + R_i + C_j + E_{ijk} + A_k + B_l + AB_{kl} + Ca_{jk} + CB_{jl} + ABC_{jkl} + E_{ijkl}$$

where i = 1...3

j = 1...3

k = 1...3

l = 1...3

Average values of the mean squares are given in table 4. A fixed effects model (i.e. A, B, and C were fixed at definite levels) was used and the null hypothesis could be tested by errors (a) and (b)[45].

TABLE 4: EXPECTED VALUES OF THE MEAN SQUARES FOR A SPLIT PLOT MODEL IN A RANDOMIZED COMPLETE BLOCK DESIGN

Source	df	Expected MS (fixed model)
Blocks	r-1	$\sigma\varepsilon^2 + ab\sigma^2_\delta + abc\sigma^2Bl$
C (Temp)	c-1	$\sigma\varepsilon^2 + ab\sigma^2_\delta + rab\sigma^2C$
Error (a)	(r-1) (c-1)	$\sigma\varepsilon^2 + ab\sigma^2_\delta$
A	(a-1)	$\sigma\varepsilon^2 + rbc\sigma^2A$
B	(b-1)	$\sigma\varepsilon^2 + rac\sigma^2B$
AB	(a-1) (b-1)	$\sigma\varepsilon^2 + rc\sigma^2AB$
CA	(c-1) (a-1)	$\sigma\varepsilon^2 + rb\sigma^2CA$
CB	(c-1) (b-1)	$\sigma\varepsilon^2 + ra\sigma^2CB$
ABC	(a-1) (b-1) (c-1)	$\sigma\varepsilon^2 + r\sigma^2ABC$
Error (b)	2c(b-1) (a-1) (r-1)	$\sigma\varepsilon^2$

5.2.2 Collection of Sample Material

A square plot (18 x 18 feet) was marked on a level strip of summerfallow at the Ellerslie experimental farm. All vegetation was removed and the soil was roto-tilled to a depth of about six inches. The plot was further divided into 81 two-foot squares (i.e. the number of samples required for the experiment).

A system of randomization was used which involved numbering each square in the plot and randomizing by means of a table of random numbers. Samples were collected as required in the experiment according to the randomized order. This was done to eliminate the effect of any gradient or boundary condition which might exist on the sample plot.

The soil in this area was classified as a loam. Some of the

physical properties and moisture constants had been determined[21,34] and are included in Appendix II.

5.2.3 Sample Preparation

Each sample consisted of approximately twenty pounds of soil (wet weight) when removed from the test plot. Samples were procured in lots of nine since this was the number of moisture-density combinations to be frozen at a particular temperature in any replicate. The sample material was put through a No. 4 mesh sieve to remove stones, coarse root material and some of the larger aggregates. The screened samples were placed in a drying bin and dried until their moisture content was below 15 percent (dry basis). Approximately 200 g of soil was taken from each sample and placed in a drying oven to obtain an accurate moisture determination. The remainder of each sample was immediately placed in a sealed plastic bag to prevent further moisture loss.

Data from the moisture determinations were used to calculate the number of grams of water needed to bring the samples to the required moisture contents of 15, 25 or 35 percent. The water and soil were thoroughly mixed with a beater (figure 16) driven by an electric drill.

After moisturizing each sample was placed in a sample tube and compacted to 60, 70 or 80 pcf. The weight of moist soil and the amount of compactive effort required for each moisture-density combination were calculated prior to sample preparation. All samples were seven inches in height because thicker soil layers resulted in extremely low count rates from the amerecium source at high mass thickness.

A modified Proctor hammer with a five-inch diameter foot (figure 17) was used to compact the samples. Compacted samples were placed in sealed plastic bags for 48 hours to allow moisture to

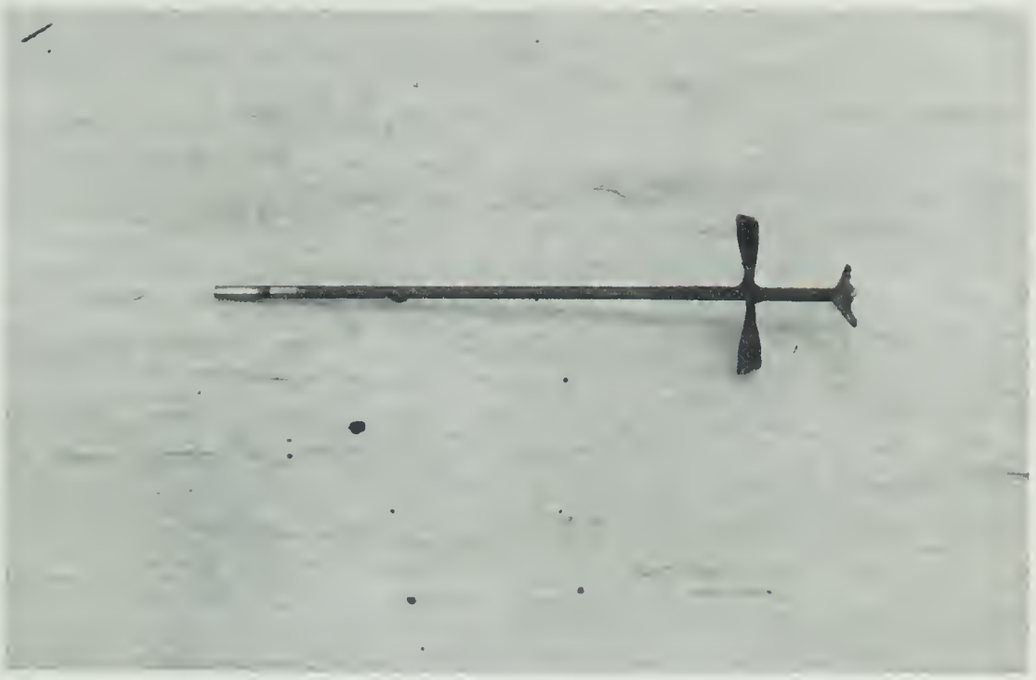

Figure 16: Soil mixer.

Figure 17: Modified Proctor hammer.

equilibrate before measurements were taken.

5.2.4 Moisture-Density Measurement

All sample thicknesses were measured and recorded before count rates were taken with the radiation equipment. The nine samples in each run were completely randomized to eliminate the effect of any gradient which might exist over time in the measuring equipment. Each sample tube was placed in the probe unit as shown in figure 18 and two one-minute counts taken.

When count rates had been recorded for all samples, the second source was installed on the probe unit and the entire counting process repeated.

5.2.5 Standardized Procedures

Variations in counting rate caused by temperature changes and high voltage drift were minimized by establishing a definite operating procedure including a method of standardizing count rates. The steps in this procedure were followed throughout the experiment and are outlined below:

i) A warm up period of 20 minutes allowed the components of the system to reach a stable operating temperature.

ii) The high voltage supply to the detector was set at the required level.

iii) Pulse height analyzer window height and width were set.

iv) Two one-minute counts were taken through the counting standard (section 5.1.4). If these counts were within acceptable limits, their values were recorded. Otherwise steps ii) and iii) were repeated.

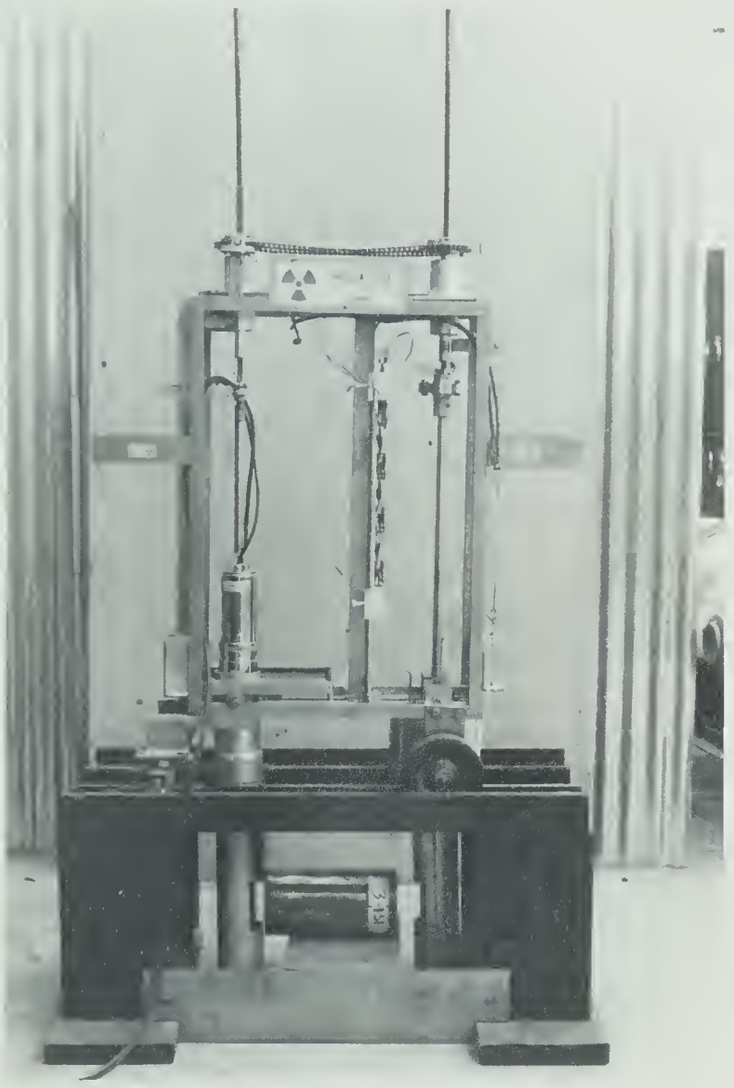

Figure 18: Sample in measuring position.

v) Following the standard count, two one-minute counts were taken through a sample and recorded.

vi) The next sample was placed in the machine and steps iv) and v) were repeated until all samples had been counted.

5.2.6 Freezing Procedure

Each sample tube was placed in a six inch diameter plastic container which was filled to a depth of about four inches with soil at the same moisture and density as the sample. The sample was separated from the soil in this container by a porous paper membrane. In this way, moisture was free to migrate to or from the sample as the frost front advanced.

The soil samples were placed in special insulated containers for the freezing part of the experiment. Each container consisted of a five-gallon pail with a removable plastic cover (figure 19). Loose-fill insulation was poured around the sample until the pail was filled. The plastic cover was tied in place leaving only the top of the sample tube exposed. The purpose of these insulated containers was to duplicate field conditions more closely by producing a uni-directional freezing front.

Thermocouples were installed at depths of two, four and six inches from the surface of all samples in the first replicate (figure 20). A continuous recording of the temperature was made during freezing to monitor the movement of the frost front and to determine the length of time required to completely freeze each sample.

Three freezing temperatures (+10, -5 and -20 degrees Fahrenheit) were used in the experiment. The order in which these temperature

Figure 19: Insulated sample container.

Figure 20: Thermocouples installed in sample tube.

levels were used was randomized in each replicate.

5.2.7 Thawing and Re-Measuring

At the end of the freezing period, the samples were allowed to thaw at room temperature before being removed from the insulated containers. During the thawing process, the exposed ends of the sample tubes were covered with plastic bags to minimize moisture loss through evaporation. The thickness of each thawed sample was measured and recorded and moisture-density measurements were taken as described in section 5.2.4.

5.2.8 Data Processing

A program was written in Fortran IV (Appendix III) to solve the following set of simultaneous equations for dry bulk density (Ps) and moisture content (Pw):

$$\ln I = \ln Io - (\mu s Ps + \mu w Pw)X. \quad (5.1)$$

$$\ln I' = \ln I'o - (\mu' s Ps + \mu' w Pw)X. \quad (5.2)$$

where I = count rate through sample (cesium source)

Io = unattenuated count rate (cesium source)

μs = mass attenuation coefficient for soil (cesium source)

μw = mass attenuation coefficient for water (cesium source)

I' = count rate through sample (amerecium source)

I'o = unattenuated count rate (amerecium source)

$\mu' s$ = mass attenuation coefficient for soil (amerecium source)

$\mu' w$ = mass attenuation coefficient for water (amerecium source)

X = sample length (cm).

Substituting the values for I, I', Io, I'o, μs, $\mu' s$, μw, $\mu' w$ determined in the calibration process the equations become

$$\ln I = \ln (9.09 \times 10^{5}) - (0.0646Ps + 0.0690Pw)X. \quad (5.3)$$

$$\ln I' = (\ln (.180 \times 10^{7}) - (0.2724Ps + 0.1925Pw)X. \quad (5.4)$$

A correction factor for standardizing sample count rates (section 5.1.4) was also built into the computer program. Values of Ps and Pw were converted from g cm^{-3} to pounds per cubic foot (pcf) and percent respectively. A complete print-out of the experimental data is shown in Appendix IV.

The variable density change (D) was obtained by subtracting mean density after freezing $\overline{D}_2$, from mean density before freezing, $\overline{D}_1$, so that

$$Y_D = \overline{D}_1 - \overline{D}_2 \quad (5.5)$$

Two readings were taken for each sample before and after freezing and the values of $\overline{D}_1$ and $\overline{D}_2$ represent the averages of these readings.

6. RESULTS

6.1 Analysis of Variance

A split plot analysis of variance technique was used to determine which, if any, of the factors or factor interactions had a significant effect on changes in dry bulk density. Calculations were performed using a library program[14] supplied by the University of Alberta Computing Center.

Mean values of density change for the three levels of temperature, three levels of moisture and three levels of initial density are given in table 5. The analysis of variance for density change is given in table 6.

The computed F-values in the analysis of variance table indicated the temperature x initial density interaction (A x C) was significant at the .05 probability level. The significant interaction implied that differences in density in response to temperature varied with the level of initial density. The graphical illustration of the interaction (figure 21) shows the differential response of density change to initial density depending on the freezing temperature. For the highest freezing temperature, density reduction was greatest at the highest level of initial density while at the lowest temperature, density was reduced only at the highest initial density. The intermediate temperature level showed an opposite trend with density reduction greatest at the lowest initial density.

The remaining main effects and interactions shown in the analysis were not statistically significant. Although the lack of significance implied that over the ranges considered, these factors and factor

TABLE 5: MEAN DENSITY CHANGE IN POUNDS PER CUBIC FOOT FOR THE FACTORS.

Means For Temperatures

Level	Density Change
+10°F	-1.22
- 5°F	-0.66
-20°F	-0.04

Means For Moisture Contents

Level	Density Change
15%	-0.81
25%	-1.00
35%	-0.09

Means For Initial Densities

Level	Density Change
60 pcf	-0.70
70 pcf	-0.55
80 pcf	-0.66

Grand Mean = -0.64

TABLE 6: ANALYSIS OF VARIANCE FOR DENSITY CHANGE.

Source of Variation	Degrees of Freedom	Sum of Squares	Mean Squares	F
A = Temperature	2	18.65	9.33	<1
R = Replicates	2	9.99	4.99	<1
Error (a)	4	67.57	16.89	
C = Density	2	0.31	0.16	<1
B = Moisture	2	12.29	6.14	2.79
A x C	4	23.55	5.89	2.67*
A x B	4	17.40	4.35	1.98
C x B	4	12.67	3.17	1.44
A x C x B	8	8.60	1.07	<1
Error (b)	48	105.72	2.20	
Total	80	276.75		

* Significant at .05 probability level.

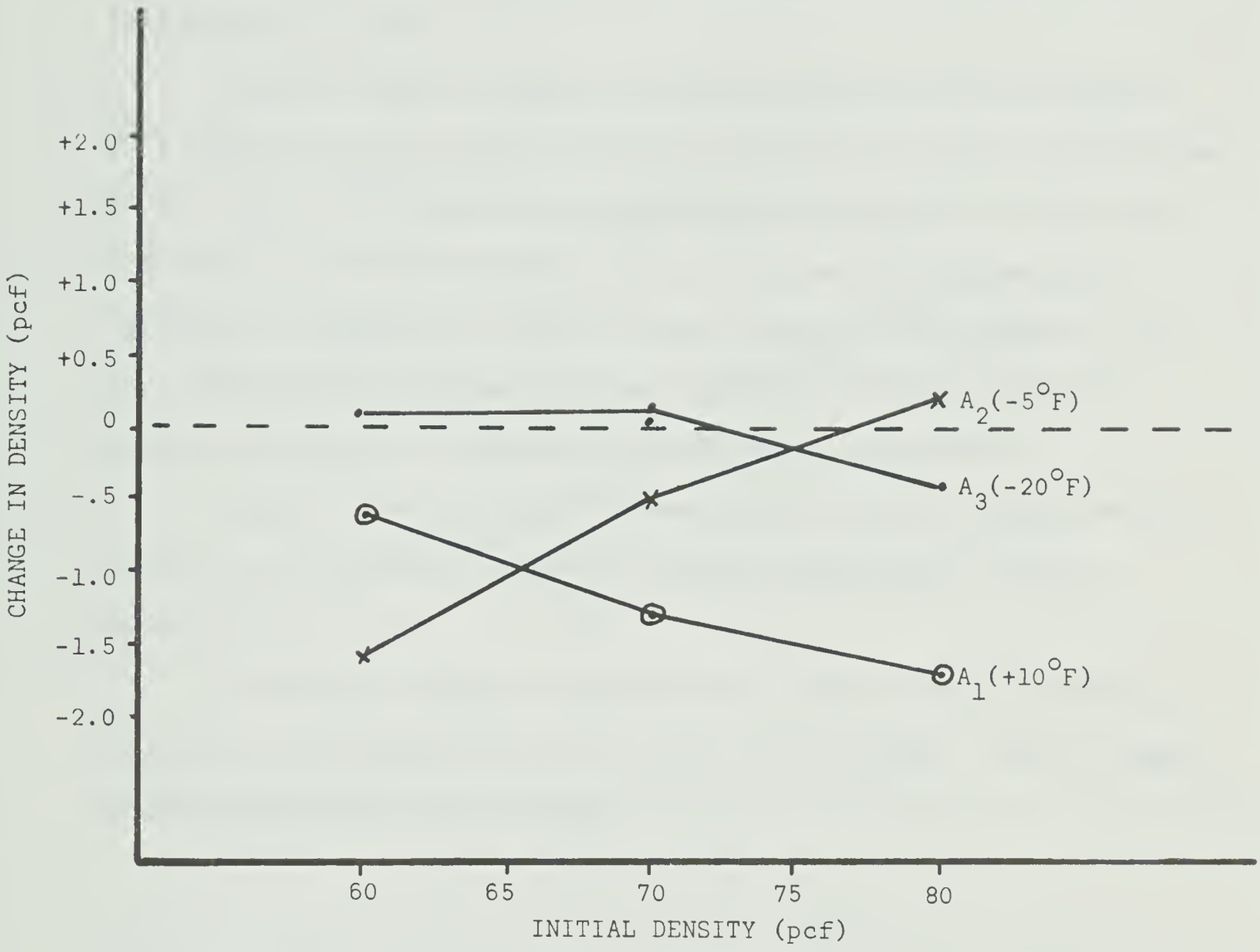

Figure 21: Graph illustrating temperature and initial density interaction.

interactions had no significant effect on changes in bulk density, certain trends may be observed. For purposes of discussion, mean density changes were plotted for the temperature x moisture interaction (A x B) and for the main effects of temperature and moisture content (figures 22, 23, 24).

From the graph in figure 22 maximum density reduction occurred at a moisture content of 25% for both the highest and lowest temperatures. At the lowest and intermediate temperatures an increase in density was indicated at a moisture content of 35%. Mean density changes at the intermediate temperature level were very similar in both figures 21 and 22. Responses were measured over all levels of moisture content in figure 21 and over all levels of initial density in figure 22.

Figure 23 indicated that decreasing the freezing temperature from +10 ^{o}F to -20 ^{o}F reduced the amount of density change from -1.22 pcf to -0.04 pcf.

The graph in figure 24 indicated that density change amounted to -0.81 pcf at 15% moisture and -1.00 pcf at 25% moisture. Density change at 35% moisture was only 0.09 pcf.

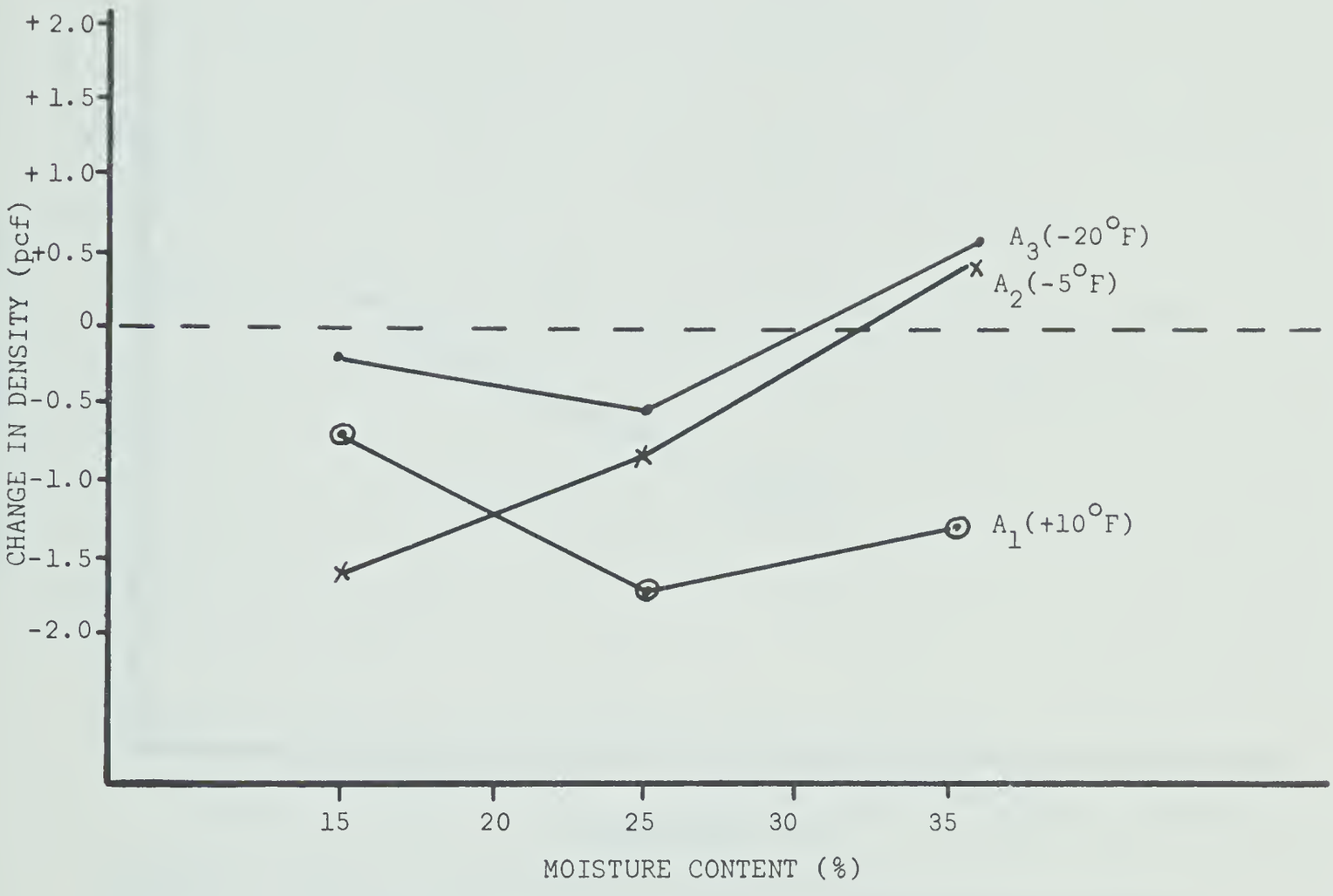

Figure 22: Graph illustrating temperature and moisture interaction.

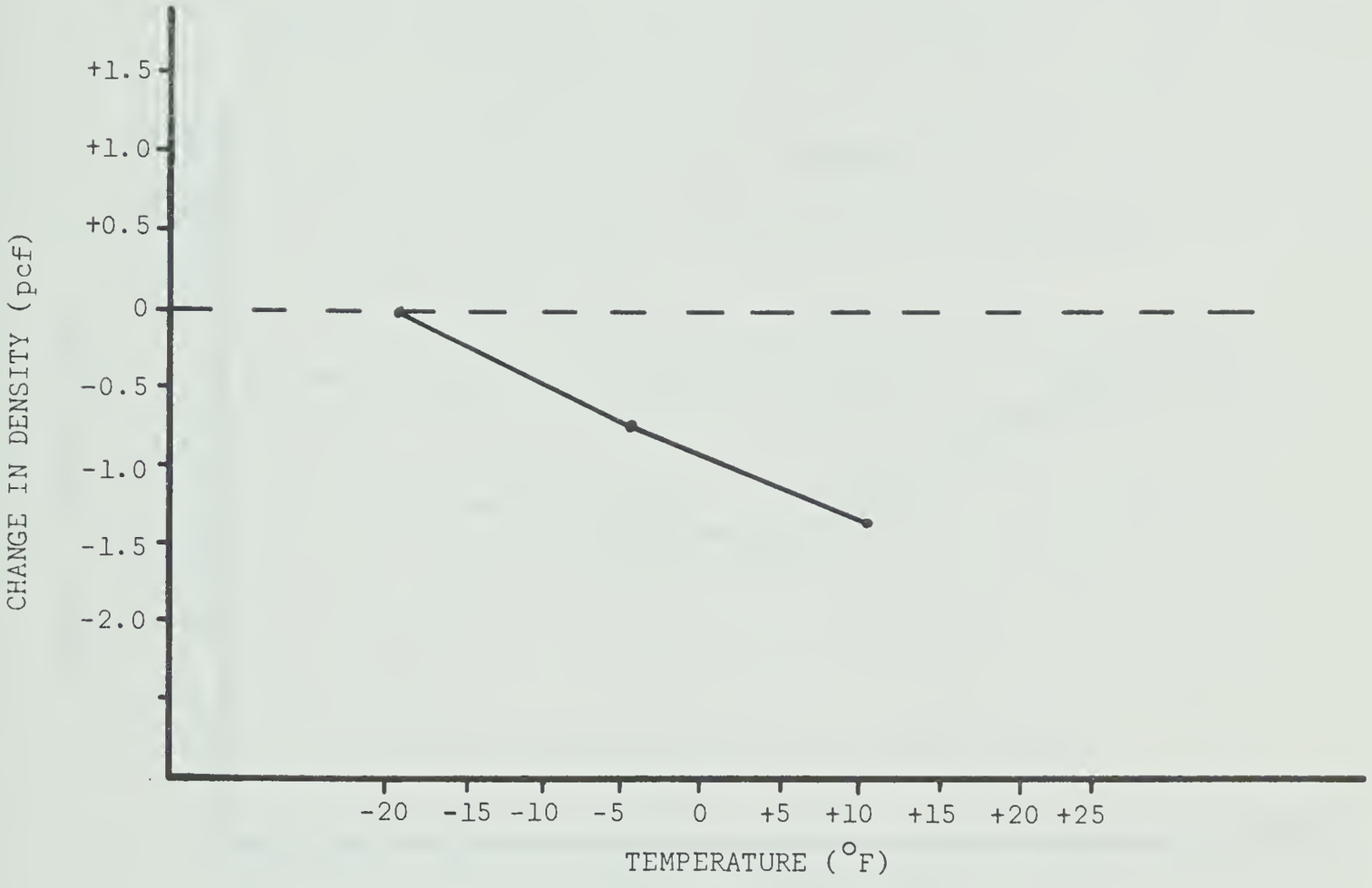

Figure 23: Graph illustrating the effect of temperature on change in density.

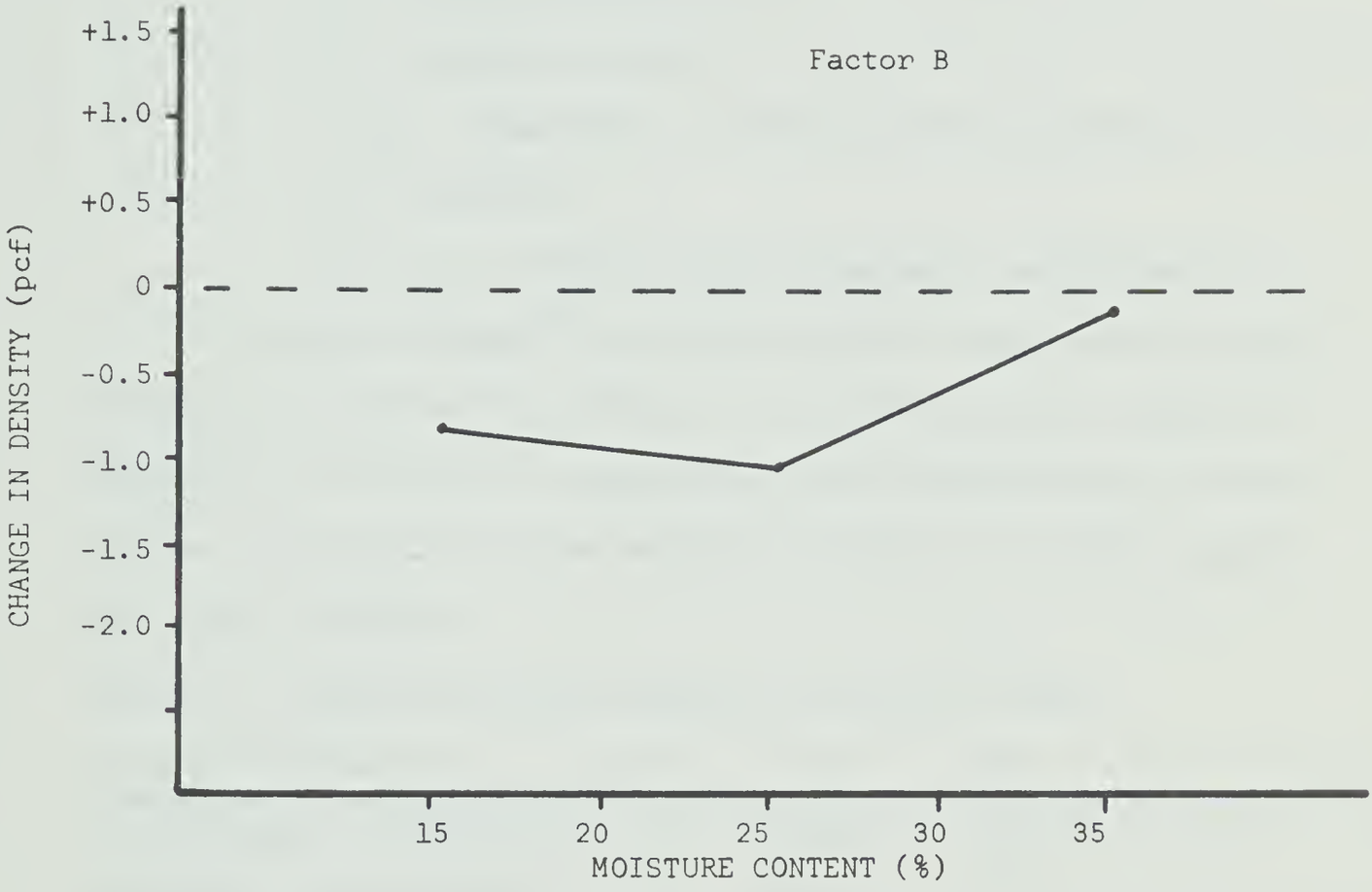

Figure 24: Graph illustrating the effect of moisture content on change in density.

6.2 Multiple Regression

It was of interest to determine the accuracy with which the two factors, temperature and moisture could be used in determining density change. A regression equation of the following form was calculated.

$$Y = A_0 + A_1X_T + A_2X_M + A_3X_M^2 + A_4X_TX_D$$

where Y = dependent variable (density change)

X_T = freezing temperature

X_M = moisture content

X_TX_D = temperature x initial density interaction

A_0 = constant

$A_1 \ldots A_4$ = multiple partial regression coefficients.

A computer program[8] for stepwise multiple regression was used. Independent variables were retained in the final multiple regression equation on the basis of a significant F-test for reduction in sum of squares. The results of the regression analysis for density change are given in table 7.

TABLE 7: REGRESSION ANALYSIS RESULTS FOR DENSITY CHANGE.

Source of Variation	DF	SS	MS	F
Attributable to Regression	4	31.95	7.99	2.49*
Deviation from Regression	76	244.81	3.22	
Total	80	276.76		

Regression Equation:

$$Y = 1.36851 - 0.25967X_T + 0.15647X_M + 0.17161X_M^2 - 0.26517X_TX_D$$

Multiple Correlation Coefficient = 0.28

Standard Error of Estimate = $\pm$ 1.83 pcf.

7. DISCUSSION OF RESULTS

7.1 Analysis of Variance

The reduction in density at a freezing temperature of +10°F (figure 23) amounted to 1.22 pcf. Although analysis of variance results indicated that this factor was not significant, a trend appeared when the three means were plotted in figure 23. The temperature treatments were applied to whole units in the split plot design and the lower precision for whole-unit comparisons[45] could partially explain the lack of statistical significance.

The trend toward greater density reduction at higher freezing temperatures is supported by Penner[37] who showed that a slower penetration of the frost line gives a higher concentration of ice in the frozen layer. Williams[61] concluded that frost heaving is caused by development of layers or lenses of ice. When freezing is rapid, ice lenses are thin since the temperature in the soil below the lense quickly drops to a point where capillary movement of water is stopped[24].

The type of freezing facility used limited the warmest temperature to +10°F. The freezing temperatures used in this experiment did not represent actual field conditions. Under field conditions, the frost front would penetrate the soil at a slower rate than at any of the temperature levels used in this study. The apparent trend shown in figure 23 indicated that at more realistic (slower) freezing rates density reduction would have been greater. This was not proven statistically and further work would be required to substantiate this evidence.

Although not statistically significant, the effect of moisture

content on density change as shown in figure 24 suggested that density change was greater at lower moisture levels. The highest moisture level (35%) is approximately field capacity for the soil used in this experiment. Water is held under less tension at this moisture content and the freezing temperature of capillary water is only slightly below $0^{o}C$. This situation does not facilitate the formation of ice lenses[24].

Although the mean for temperature had indicated a decrease in density with increasing temperature, a general statement regarding either temperature or initial density is not possible because of the interaction of temperature x initial density (A x C) shown in figure 21. This interaction was due to response of density to the intermediate temperature level at the three levels of initial density. A similar trend is also shown for a temperature of $-5^{o}F$ in figure 22 where responses were measured over all levels of initial density. A satisfactory explanation for the density response at this temperature level was not possible. The two coldest temperature levels ($-5^{o}F$ and $-20^{o}F$) would produce much more rapid rates of freezing than would be encountered under actual field conditions.

Density response to a temperature of $+10^{o}F$ increased with the level of initial density (figure 21) where responses were measured over all levels of moisture content. At higher levels of initial bulk density, the amount of pore space available for ice lense development is at a minimum. Therefore, formation of ice lenses in the highly compacted samples results in greater rearrangement of the soil particles[24].

The grand mean of -0.64 pcf density change indicated values of density change obtained throughout the experiment were very small. Density changes of this magnitude would be of little practical

significance in reducing compaction in the field. However, density responses under field conditions might be very different from the responses encountered in this experiment.

7.2 Regression Analysis

The regression equation given in table 7 can be used only to describe the experimental data in terms of freezing temperature, moisture content and initial density. The practical value of the equation is limited since only 8% of the variation in Y is explained by the variables used in the equation.

7.3 Comments

Simulation of field conditions with regard to freezing rate was not accomplished in this experiment. Migration of a frost front under field conditions would depend on several factors including variations in ambient temperature, trash cover and snow cover which would be difficult to simulate in the laboratory. The results of this experiment suggested (although statistical evidence was lacking) that the slower rates of freezing encountered in the field would produce greater changes in bulk density.

The ranges of moisture and density considered in the experiment included moisture and density conditions which could be expected on the plot of land from which the sample material was collected (see Appendix II).

8. CONCLUSIONS

The following conclusions can be drawn from this investigation:

1. Non-destructive measurement of soil bulk density and moisture content can be achieved using dual-energy gamma transmission techniques.
2. The scintillation detector system was highly sensitive to high voltage changes and variations in ambient temperature.
3. Significant density changes were caused by an interaction of the parameters temperature x initial density.
4. Freezing temperatures that would simulate field conditions were not obtained in this research. A trend in the data suggested that greater reduction in bulk density would be achieved at slower freezing rates.
5. Density changes due to the levels of the factors studied in this experiment were small, indicating little loosening of compacted soil during a freeze-thaw cycle.
6. Prediction of density responses in the field would not be possible on the basis of results obtained in this experiment.

7. With minor modifications, the present detection system could be used in a field experiment to assess the effect of freeze-thaw cycles on a soil in-situ.

9. RECOMMENDATIONS

On the basis of information obtained during this investigation several general recommendations may be made.

1. The accuracy of moisture-density measurements could be improved by increasing the stability of the high voltage power supply. Slight drift in the power supply necessitated frequent calibration checks throughout the experiment.
2. Count rates from the detector were influenced by ambient temperature changes. A temperature compensating system would improve the overall accuracy, particularly if the instrument were used for a field experiment where wide variations in temperature would be encountered.
3. The gamma sources used in this experiment were partially collimated. It was found that collimation was not necessary when a pulse height analyzer was used in the counting system. This factor should be considered in the design of similar equipment.
4. Future laboratory studies involving frost action should be designed to include freezing rates more comparable to those encountered in the field.

10. BIBLIOGRAPHY

1. Alboaba, F.O. 1969. Effects of Time on Compaction of Soils by Rollers. Transactions of the A.S.A.E., 12: (3), 302-304.

2. Bateman, H.P. 1963. Effects of Field Machine Performance on Soil Physical Properties and Crop Response. Transactions of the A.S.A.E., 6: (1), 19-25.

3. Baver, L.D. 1956. Soil Physics. 3 ed. John Wiley and Sons, Inc., New York.

4. Bekker, M.G. 1961. Mechanical Properties of Soil and Problems of Compaction. Transactions of the A.S.A.E., 4: (2), 231-234.

5. Blatz, H. 1964. Introduction to Radiological Health. McGraw-Hill Book Company, New York.

6. Bourget, S.J., Kemp, J.G. and Dow, B.K. 1961. Effect of Tractor Traffic on Crop Yields and Soil Density. Agric. Engng., 42: (10), 554.

7. Bowers, W. and Bateman, H.P. 1960. Research Studies of Minimum Tillage. Transactions of the A.S.A.E. 3: (2), 1-3, 12.

8. Buttuls, P. 1969. Stepwise Multiple Regression Library Program. Department of Computing Science, University of Alberta, Edmonton.

9. Chancellor, W.J. and Schmidt, R.H. 1962. A Study of Soil Deformation Beneath Surface Loads. Transactions of the A.S.A.E., 5: 240-246, 249.

10. Chase, G.D. 1960. Principles of Radioisotope Methodology. Burgess Publishing Company, Minneapolis.

11. Cooper, A.W. and Nichols, M.L. 1959. Some Observations on Soil Compaction Tests. Agric. Engng., 40: (5), 264-267.

12. Domier, K.W. 1964. A Preliminary Look at Soil Compaction on Osborne Clay Soil. Unpublished paper, Department of Agricultural Engineering, University of Manitoba, Winnipeg.

13. Doneen, L.D. and Henderson, D.W. 1953. Compaction of Irrigated Soils by Tractors. Agric. Engng., 34: (2), 94-95, 102.

14. Easton, M. 1968. Analysis of Variance Library Program. Department of Computing Science, University of Alberta, Edmonton.

15. Eavis, B.W. 1967. Mechanical Impedance and Root Growth. Paper No. 4/F/39, presented at the Agric. Engng. Symp. of the Inst. of Agric. Engng.

16. Feldman, M. 1968. Wheel Traffic Effects on Soil Compaction and Growth of Wheat. MSc. Thesis, Department of Agricultural Engineering, University of Manitoba, Winnipeg.

17. Free, G.R. 1953. Traffic Soles. Agric. Engng., 34: 528-531.

18. Gardner, W.H. and Fischer, M.E. 1966. Concurrent Measurement of Bulk Density and Water Content of Soil Using Two Gamma Ray Energies. Amer. Soc. Agron., Agron. Abstracts, 46.

19. Gill, W.R. 1959. Soil Compaction by Traffic. Agric. Engng., 40: 392-394, 400, 402.

20. Gurr, C.G. 1962. Use of Gamma Rays in Measuring Water Content in Unsaturated Columns of Soil. Soil Sci., 94: (4), 224-229.

21. Heapy, L. 1970. Personal Communication. Department of Soil Science, University of Alberta, Edmonton.

22. Jamison, V.C., Weaver, H.A. and Reed, I.F. 1950. The Distribution of Tractor Tire Compaction Effects in Cecil Clay. Soil Sci. Soc. Amer. Proc., 15: 34-37.

23. Johnson, W.H. and Taylor, G.S. 1960. Tillage Treatment for Corn on Clay Soils. Transactions of the A.S.A.E., 3: (2), 4-7, 10.

24. Kohnke, H. 1968. Soil Physics. McGraw-Hill Book Company, New York, 129-132, 185-186.

25. Kucera, H.L. and Promersberger, W.J. 1960. Soil Compaction - a North Dakota Problem? North Dakota Bi-Monthly Research Bulletin, 21: (7).

26. Lal, R. 1967. A Laboratory Study of the Effect of Agricultural Land Packers on Soil. Ph.D. Thesis, Department of Agricultural Engineering, University of Saskatchewan, Saskatoon.

27. Lambe, T.W. 1958. The Structure of Compacted Clay. Jour. of Soil Mechanics and Foundations, Amer. Soc. of Civ. Engng., 84: (SM2)

28. Ligon, J.T. 1969. Evaluation of the Gamma Transmission Method for Determining Soil Water Balance and Evapotranspiration. Transactions of the A.S.A.E., 12: (1), 121-126.

29. Luttrell, D.H., Bockhop, C.W. and Lovely, W.G. 1964. The Effect of Tillage Operations on Soil Physical Conditions. A.S.A.E. Paper No. 64-103.

30. McHenry, J.R. 1964. A Two-Probe Nuclear Device for Determining the Density of Sediments, Intl. Assoc. Sci. Hydrol., Publ. 65: 189-202.

31. McHenry, J.R. and Dendy, F.E. 1964. Measurement of Sediment Density by Attenuation of Transmitted Gamma Rays. Soil Sci. Soc. Amer. Proc. 28: 817-822.

32. Morgan, K.Z. and Turner, J.E. 1967. Principles of Radiation Protection. John Wiley and Sons Inc., New York.

33. Morton, C.T., Stout, B.A., Buchele, W.F. and Snyder, F.W. 1960. The Effect of Soil Physical Condition on Energy Requirements for Simulated Seedling Emergence and Actual Emergence. Paper presented at eleventh general meeting, Amer. Soc. of Sugar Beet Technologists.

34. Pawluk, S. 1970. Personal Communication. Department of Soil Science, University of Alberta, Edmonton.

35. Penner, E. 1969. Particle Size as a Basis for Predicting Frost Action in Soils. Research Paper No. 406, Division of Building Research, National Research Council of Canada.

36. Penner, E. 1968. Heaving Pressure in Soils During Unidirectional Freezing. Research Paper No. 347, Division of Building Research, National Research Council of Canada.

37. Penner, E. 1961. The Importance of Freezing Rate in Frost Action in Soils. Research Paper No. 126, Division of Building Research, National Research Council of Canada.

38. Phillips, R.E., Jensen, C.R. and Kirkham, D. 1960. Use of Radiation Equipment for Plow Layer Density and Moisture. Soil Science 89: (1).

39. Phillips, R.E. and Kirkham, D. 1962. Soil Compaction in the Field and Corn Growth. Agronomy Jour. 54: 29-34.

40. Pierpoint, G. 1965. Measuring Surface Soil Moisture With the Neutron Depth Probe and Surface Shield. Soil Sci. 101: (3), 189-192.

41. Reginato, R.J. and Van Bavel, C.H.M. 1964. Soil Water Measurement with Gamma Attenuation. Soil Sci. Soc. Amer. Proc., 28: 721-724.

42. Smith, E.M., Taylor, T.H. and Smith, S.W. 1967. Soil Moisture Measurement Using Gamma Transmission Techniques. Transactions of the A.S.A.E., 10: (2), 205-208.

43. Soane, B.D. 1967. Double Energy Gamma Transmission for Moisture and Density Measurement in Soil Tillage Studies. Paper submitted to International Soil Water Symposium, Czech. National Committee, International Commission on Irrigation and Drainage, Prague.

44. Soane, B.D. 1967. Dual Energy Gamma Ray Transmission for Coincident Measurement of Water Content and Dry Bulk Density of Soil. Nature, Vol. 214, No. 5094, pp 1273-1274.

45. Steele, R.G.D. and Torrie, J.H. 1960. Principles and Procedures of Statistics. McGraw Hill Book Company Inc., New York.

46. Stone, J.F., Kirkham, D. and Read, A.A. 1955. Soil Moisture Determination by a Portable Neutron Scattering Moisture Meter. Soil Sci. Soc. Amer. Proc. 19: 419 - 423.

47. Stout, B.A., Buchele, W.F. and Snyder, F.W. 1961. Effect of Soil Compaction on Seedling Emergence under Simulated Field Conditions. Agric. Engng. 42: (2), 68-71, 87.

48. Swamy Rao, A.A., Hay, R.C. and Bateman, H.P. 1960. Effect of Minimum Tillage on Physical Properties of Soils and Crop Response. Transactions of the A.S.A.E., 3: (2), 8-10.

49. Terry, C.W. and Wilson, H.M. 1953. The Soil Penetrometer in Soil Compaction Studies. Agric. Engng., 34: (12), 831-834.

50. Van Bavel, C.H.M. 1959. Soil Densitometry by Gamma Transmission. Soil Sci. 87: 50-58.

51. Van Bavel, C.H.M., Underwood, N. and Ragar, S.R. 1957. Transmission of Gamma Radiation by Soils and Soil Densitometry. Soil Sci. Soc. Amer. Proc., 21: 588-591.

52. Vandenberg, G.E. and Gill, W.R. 1962. Pressure Distribution Between a Smooth Tire and the Soil. Transactions of the A.S.A.E., 5: (2), 105-107.

53. Van Doren Jr., D.M., Brown, W.N. and Johnson, W.H. 1964. Soil Compaction and Crop Growth. O.A.E.S. Misc. Ohio.

54. Veihmeyer, F.J. and Hendrickson, A.H. 1948. Soil Density and Root Penetration. Soil Sci., 65: 487-493.

55. Vomocil, J.A. 1954. In Situ Measurement of Bulk Density of Soil by Gamma Ray Absorption Technique. Soil Sci., 77: 341-342.

56. Vomocil, J.A. and Flocker, W.J. 1961. Effect of Soil Compaction on Storage and Movement of Soil, Air and Water. Transactions of the A.S.A.E., 4: (2), 242-246.

57. Vomocil, J.A., Fountaine, E.R. and Reginato, R.J. 1958. The Influence of Speed and Drawbar Load on the Compacting Effect of Wheeled Tractors. Soil Sci. Soc. Amer. Proc., 22: 178-180.

58. Wang, C.H. and Willis, D.L. 1965. Radiotracer Methodology in Biological Science. Prentice-Hall Inc., New Jersey.

59. Weaver, H.A. 1950. Tractor Use Effects on Volume Weight of Davidson Loam. Agric. Engng., 31: 182-183.

60. Weaver, H.A. and Jamison, V.C. 1951. Effects of Moisture on Tractor Tire Compaction of Soil. Soil Sci., 71: 15-23.

61. Williams, P.J. 1968. The Nature of Freezing Soil and its Field Behavior. Norwegian Geotechnical Institute, Publication No. 72, pp. 91-119.

11. APPENDICES

Appendix I: Calibration Data for Amerecium and Cesium Sources.

1. Amerecium.

a) Count Rate Data for Soil.

Mass Thickness, X g cm^{-2}	Standardized Count Rate (cpm)	log cpm, Y
15.62	267,833	5.42782
17.48	156,506	5.19450
19.38	89,851	4.95352
20.89	58,378	4.76626
21.92	43,378	4.63729
22.98	33,286	4.52361
24.12	24,872	4.39569
25.60	18,468	4.26642

Regression Equation:

$$\log Y = 7.2548 - 0.1183 X$$

b) Count Rate Data for Water

Mass Thickness, X $g\ cm^{-2}$	Standardized Count Rate (cpm)	log cpm, Y
18.39	524,911	5.72008
19.44	422,990	5.62634
20.48	352,158	5.54678
21.53	301,262	5.47900
22.57	236,648	5.37402
23.62	182,851	5.26197
24.66	150,462	5.17751
25.71	127,960	5.10680
26.75	108,987	5.03743

Regression Equation:

$$\log Y = 7.25658 - 0.08358\ X$$

c) Amerecium Calibration Curves for Soil and Water

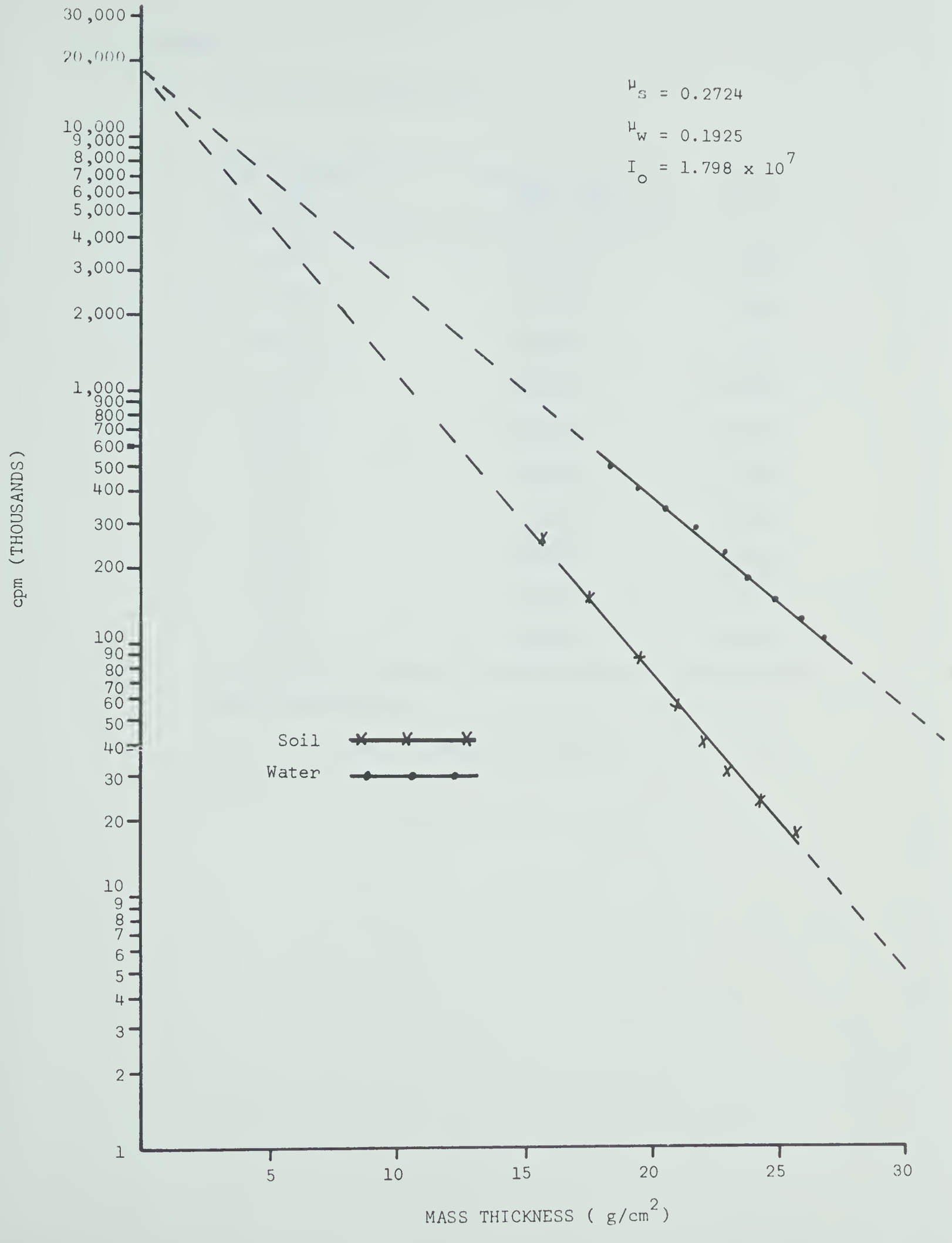

2. Cesium

a) Count Rate Data for Soil.

Mass Thickness, X g cm^{-2}	Standardized Count Rate (cpm)	log cpm, Y
13.38	385,819	5.58636
14.84	348,250	5.54183
16.30	314,823	5.49803
17.76	289,767	5.46212
19.23	260,074	5.41513
20.69	241,868	5.38361
22.15	219,718	5.34184
23.62	198,008	5.29667
25.08	180,287	5.25598
26.54	163,022	5.21219

Regression Equation:

$$\log Y - 5.95903 - 0.02804 X$$

b) Count Rate Data for Water

Mass Thickness, X g cm^{-2}	Standardized Count Rate (cpm)	log cpm, Y
15.26	301,804	5.47971
16.30	281,240	5.44901
17.35	263,062	5.42012
18.39	243,495	5.38650
19.44	228,646	5.35909
20.48	205,455	5.31260
21.53	196,979	5.29447
22.57	184,157	5.26530
23.62	167,858	5.22480
24.66	159,285	5.20223
25.71	146,698	5.16641

Regression Equation:

$$\log Y = 5.93773 - 0.02998 X$$

c) Cesium Calibration Curves for Soil and Water

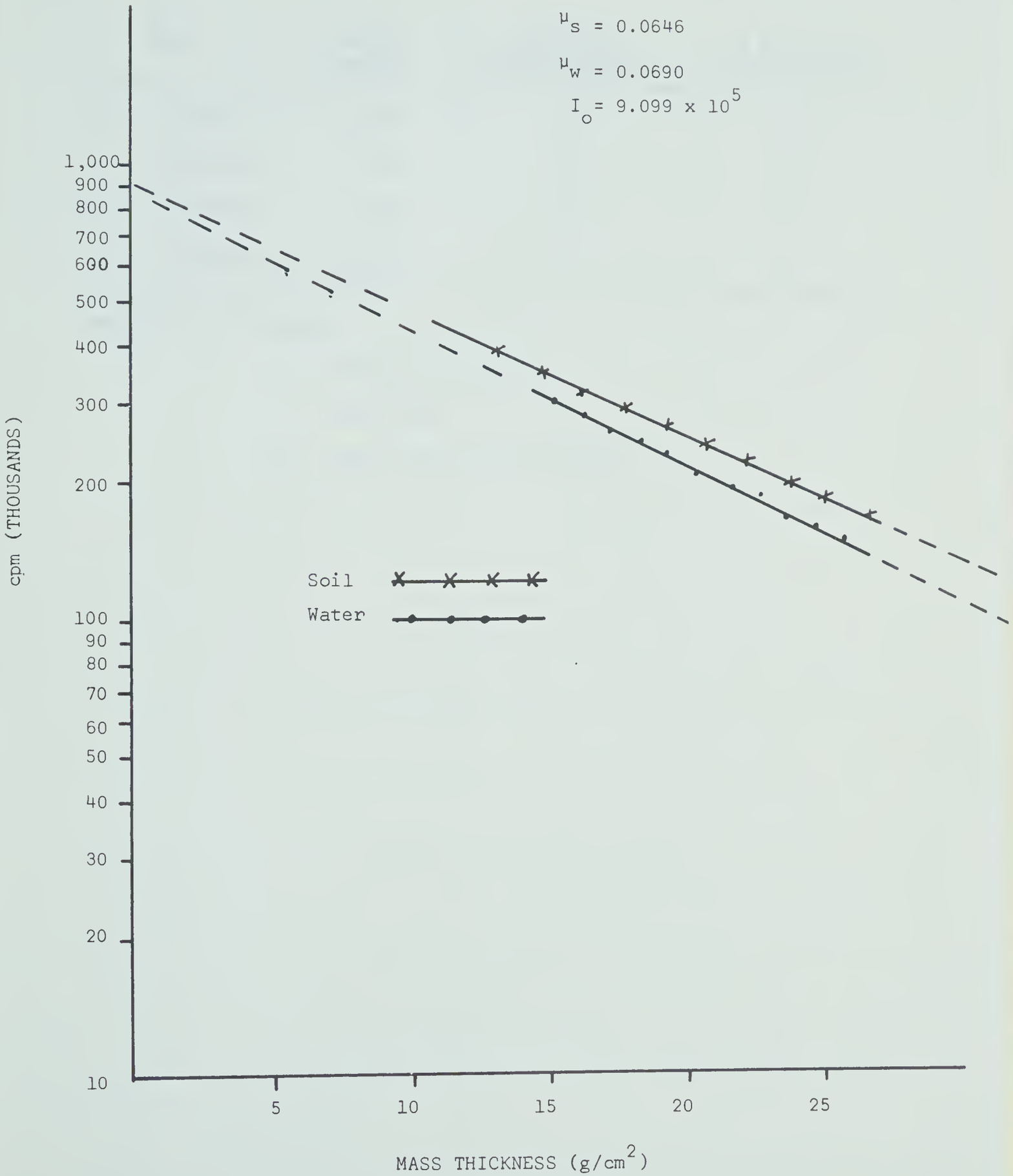

Appendix II: Some Properties of Ellerslie Loam.

Depth	Bulk Density	% Moisture at Field Capacity	% Moisture at Wilting Point
0 - 6 inches	1.00	35.5	19.5
6 - 12 inches	1.10	31.2	17.5
12 - 24 inches	1.59	27.6	14.0
24 - 36 inches	1.64	27.6	13.5

Dominant clay minerals:

40 - 60% montmorillorite

30% illite

10 - 30% kaolinite and feldspars

```
C IA = ACTUAL AM. COUMT
C IC = ACTUAL CS. COUNT
C IZA = ZERO MASS THICKNESS COUNT FOR AM.
C IZC = ZERO MASS THICKNESS COUNT FOR CS.
C SCMA = STANDARD COUNT MEAN FOR AM. , SCMC = FOR CS.
C SCA = STANDARDIZING COUNT FOR AM. , SCC = FOR CS.
C USA = SOIL SLOPE FOR AM. , USC = FOR CS.
C UWA = WATER SLOPE FCR AM. , UWC = FOR CS.
C IAS = STANDARDIZED COUNT FOR AM. , ICS = FOR CS.
C X = HEIGHT OF SAMPLE , Y = SAMPLE NUMBER
C DGM = CALCULATED SOIL DENSITY IN GM/CC
C DLB = CALCULATED SOIL DENSITY IN LB/FT3
C MC = MOISTURE CONTENT
C SAMP = SAMPLE DESIGNATION
      REAL*4 SAMP
      INTEGER*2 SAMQ
      REAL IZA,IZC,IA,IC,IAS,ICS,MC
      INTEGER Y
      USA = 0.2724
      UWA = 0.1925
      USC = 0.0646
      UWC = 0.0690
      IZA = 17980000.
      IZC = 909910.
      SCMA = 78346.
      SCMC = 277932.
      Y=1
      WRITE(6,41)
   41 FORMAT(//////,40X,'REPLICATE 1',////)
      GO TO 103
  108 WRITE(6,45)
   45 FORMAT(1H1,//////////,15X,'SAMPLE',5X,'DENSITY',7X,'MC',5X,
     1'HEIGHT',6X,'STANDARDIZED')
      GO TO 101
  102 WRITE(6,46)
   46 FORMAT(1H1,//////,40X,'REPLICATE 2',////)
      GO TO 103
  104 WRITE(6,47)
   47 FORMAT(1H1,//////,40X,'REPLICATE 3',////)
  103 WRITE(6,42)
   42 FORMAT(15X,'SAMPLE',5X,'DENSITY',7X,'MC',5X,'HEIGHT',6X,
     1'STANDARDIZED')
  101 WRITE(6,43)
   43 FORMAT(15X,'DESIG.',5X,'(LB/FT3)',6X,'(%)',6X,'(CM)',4X,'AM(CPM)
     1',4X,'CS(CPM)'//)
      J=1
  999 READ(5,51)SAMP,SAMQ,SCA,SCC,X,IA,IC
   51 FORMAT(A4,A2,4X,F6.0,4X,F7.0,4X,F5.2,4X,F6.0,4X,F7.0)
      IF(SCA.EQ.00000) GO TO 1000
C STANDARDIZE THE COUNTS
      IAS = (SCMA/SCA)*IA
      ICS = (SCMC/SCC)*IC
      MC = (ALOG(IAS/IZA)-ALOG(ICS/IZC)*(USA/USC))/(X*UWC*(USA/USC)
     1-X*UWA)
      DGM = (ALOG(IAS/IZA)+X*MC*UWA)/(-X*USA)
      DLB = DGM*62.3
```

```
      MC = (MC/DGM)*100
      WRITE(6,44)SAMP,SAMQ,DLB,MC,X,IAS,ICS
   44 FORMAT(15X,A4,A2,6X,F6.3,6X,F6.3,3X,F5.2,3X,F7.0,4X,F8.0)
      Y=Y+1
      J=J+1
      IF(J.EQ.41) GO TO 108
      IF(Y.EQ.55) GO TO 102
      IF(Y.EQ.109) GO TO 104
      GOTO 999
1000  STOP
      END
```

Appendix IV: Computer Print-Out of Experimental Data.

REPLICATE 1

SAMPLE DESIG.	DENSITY (LB/FT3)	MC (%)	HEIGHT (CM)	STANDARDIZED AM(CPM)	STANDARDIZED CS(CPM)
1-111U	58.006	21.907	17.53	105916.	247705.
1-111F	57.084	22.364	17.65	109444.	249397.
1-211U	55.742	24.815	17.78	110347.	247961.
1-211F	58.829	16.254	17.78	109754.	254792.
1-311U	57.238	20.636	17.91	105749.	248655.
1-311F	58.981	15.913	18.03	101941.	250443.
1-121U	57.209	30.303	17.78	81216.	225255.
1-121F	57.507	27.440	17.78	86439.	230992.
1-221U	59.198	26.024	17.65	80511.	227871.
1-221F	59.167	25.204	17.65	82900.	230206.
1-321U	58.124	25.212	17.91	84298.	231186.
1-321F	57.412	27.457	18.03	80861.	227055.
1-131U	67.405	28.405	16.76	47749.	197656.
1-131F	65.180	32.762	16.76	50134.	197200.
1-231U	66.880	30.500	17.02	42404.	190285.
1-231F	67.963	28.605	17.02	41140.	190081.
1-331U	67.281	31.200	16.51	47907.	195917.
1-331F	67.713	32.557	16.51	44007.	190762.
1-112U	70.530	14.426	17.78	42732.	202890.
1-112F	70.084	14.791	17.78	43777.	203795.
1-212U	72.695	12.136	17.65	40682.	202440.
1-212F	72.968	11.741	17.65	40394.	202441.
1-312U	71.614	11.194	17.91	42323.	205279.
1-312F	72.488	10.807	17.91	39925.	202708.
1-122U	74.325	19.579	17.40	28790.	179813.
1-122F	72.096	22.662	17.53	29549.	178688.
1-222U	71.979	20.807	17.78	29327.	179719.
1-222F	73.937	16.389	17.78	29469.	183386.
1-322U	74.241	18.688	17.40	30050.	182452.
1-322F	72.732	22.213	17.40	29813.	179421.
1-132U	75.853	35.106	16.76	17451.	148536.
1-132F	76.152	34.019	16.76	17724.	149762.
1-232U	73.470	35.516	17.27	17406.	148202.
1-232F	77.428	28.136	17.27	16247.	149924.
1-332U	78.124	28.446	16.76	18563.	154956.
1-332F	76.658	34.410	16.64	17522.	149088.
1-113U	78.386	14.745	18.29	17729.	162813.
1-113F	75.159	19.436	18.42	18399.	160740.
1-213U	80.874	16.202	17.40	18910.	164298.
1-213F	79.508	18.959	17.40	18872.	162121.

SAMPLE DESIG.	DENSITY (LB/FT3)	MC (%)	HEIGHT (CM)	STANDARDIZED AM(CPM)	CS(CPM)
1-313U	79.737	12.507	18.16	18285.	165882.
1-313F	77.696	16.357	18.29	17556.	161158.
1-123U	82.849	24.936	17.14	12109.	140993.
1-123F	80.682	28.195	17.14	12752.	140831.
1-223U	83.338	26.309	16.76	12864.	142314.
1-223F	82.982	27.236	16.76	12751.	141415.
1-323U	81.696	32.028	17.40	8801.	125852.
1-323F	78.585	35.451	17.65	9143.	125275.
1-133U	75.453	42.736	18.03	7786.	116605.
1-133F	74.978	43.704	18.03	7851.	116423.
1-233U	71.951	49.368	18.03	8550.	116614.
1-233F	76.087	41.150	17.91	8215.	119014.
1-333U	78.880	35.464	17.91	7940.	120729.
1-333F	77.403	39.691	17.78	8100.	119264.

REPLICATE 2

SAMPLE DESIG.	DENSITY (LB/FT3)	MC (%)	HEIGHT (CM)	STANDARDIZED AM(CPM)	CS(CPM)
2-111U	52.842	31.248	17.65	123786.	250503.
2-111F	53.548	29.442	17.63	122784.	251288.
2-211U	56.883	23.352	17.65	108074.	247805.
2-211F	54.281	29.048	17.65	115368.	247571.
2-311U	56.648	23.548	17.40	117930.	253210.
2-311F	55.940	24.860	17.40	120711.	253672.
2-121U	58.320	23.584	17.91	87254.	234496.
2-121F	56.304	27.080	18.03	90825.	234216.
2-221U	62.535	21.977	17.02	83140.	232907.
2-221F	57.154	32.207	17.14	93587.	232324.
2-321U	57.857	24.606	18.03	85010.	232149.
2-321F	57.067	25.322	18.16	86043.	232315.
2-131U	66.377	22.964	17.78	44673.	198230.
2-131F	65.050	27.415	17.78	42956.	193035.
2-231U	65.537	27.248	17.53	44991.	195461.
2-231F	62.318	32.989	17.78	45736.	192402.
2-331U	61.191	33.348	17.78	50346.	197034.
2-331F	62.025	31.455	17.91	47475.	195287.
2-112U	68.368	17.064	17.78	46577.	205030.
2-112F	67.486	19.266	17.78	46354.	202982.
2-212U	77.317	8.333	17.02	40625.	205897.
2-212F	73.877	14.507	17.02	41913.	201847.
2-312U	72.861	11.096	17.53	43572.	206843.
2-312F	72.763	11.599	17.53	43064.	205789.
2-122U	74.384	13.698	17.91	30209.	186760.
2-122F	71.074	19.053	18.03	31172.	183856.
2-222U	74.404	12.359	18.29	27860.	184193.
2-222F	73.488	14.514	18.16	28888.	184016.
2-322U	71.397	18.372	18.03	31115.	184305.
2-322F	72.742	15.216	18.03	31371.	187237.
2-132U	75.749	24.072	17.78	18291.	157234.
2-132F	72.594	31.683	17.78	17991.	151722.
2-232U	73.632	27.821	18.03	17307.	152581.
2-232F	72.787	29.746	18.03	17335.	151441.
2-332U	73.901	25.519	18.03	18549.	156822.
2-332F	76.385	21.355	18.03	17575.	157517.
2-113U	80.641	12.767	17.65	20334.	170075.
2-113F	79.788	14.492	17.63	20424.	168846.
2-213U	80.282	14.644	17.65	19303.	166373.
2-213F	79.284	15.616	17.65	20150.	167384.

SAMPLE DESIG.	DENSITY (LB/FT3)	MC (%)	HEIGHT (CM)	STANDARDIZED AM(CPM)	CS(CPM)
2-313U	79.637	11.837	18.29	18094.	166009.
2-313F	79.792	10.865	18.42	17764.	166076.
2-123U	82.820	15.923	18.03	12595.	148655.
2-123F	79.925	21.166	18.03	12855.	145662.
2-223U	77.665	22.212	18.42	12936.	145183.
2-223F	78.283	20.695	18.42	13066.	146586.
2-323U	82.615	15.881	18.16	12194.	147492.
2-323F	81.460	16.871	18.29	12254.	146941.
2-133U	81.909	28.679	18.03	7622.	123089.
2-133F	77.736	38.507	17.91	7791.	118619.
2-233U	77.101	40.429	17.78	8090.	118874.
2-233F	78.254	38.953	17.65	8130.	119737.
2-333U	77.961	34.302	18.29	7776.	120672.
2-333F	80.583	30.864	18.16	7411.	120991.

REPLICATE 3

SAMPLE DESIG.	DENSITY (LB/FT3)	MC (%)	HEIGHT (CM)	STANDARDIZED AM(CPM)	CS(CPM)
3-111U	56.789	21.719	18.03	102813.	245999.
3-111F	56.969	21.144	18.03	103015.	246594.
3-211U	56.652	20.850	17.78	114880.	253732.
3-211F	50.931	34.779	17.91	125006.	248670.
3-311U	57.704	24.833	17.02	115490.	250846.
3-311F	57.154	26.285	17.02	116009.	250006.
3-121U	57.750	25.455	17.91	86588.	232588.
3-121F	57.479	26.301	17.91	86421.	231831.
3-221U	57.425	29.842	17.53	87121.	229709.
3-221F	56.804	28.742	17.65	92105.	233830.
3-321U	57.856	25.704	17.91	85065.	231346.
3-321F	57.359	27.430	17.78	87659.	231833.
3-131U	60.530	30.907	17.91	55792.	204003.
3-131F	60.977	29.703	18.03	53565.	202687.
3-231U	64.390	26.544	17.91	45095.	196076.
3-231F	62.990	28.226	18.03	46559.	196501.
3-331U	64.100	27.170	17.78	47323.	198069.
3-331F	65.353	27.632	17.53	45137.	195353.
3-112U	72.586	11.031	17.53	44690.	208196.
3-112F	72.737	10.891	17.53	44378.	207968.
3-212U	73.218	9.571	17.78	41263.	205505.
3-212F	71.104	12.080	17.91	42673.	204892.
3-312U	72.718	12.255	17.40	44058.	206355.
3-312F	73.010	12.674	17.40	42305.	203922.
3-122U	74.634	14.555	17.78	29908.	185575.
3-122F	73.906	14.813	17.91	30072.	185611.
3-222U	73.813	16.060	17.91	28811.	182621.
3-222F	72.223	16.630	18.03	31008.	185536.
3-322U	71.243	18.788	18.03	31029.	183851.
3-322F	72.918	16.073	17.91	31133.	186177.
3-132U	76.499	20.529	17.91	18865.	160959.
3-132F	75.017	22.708	18.03	18805.	159285.
3-232U	76.346	21.259	17.91	18545.	159742.
3-232F	74.369	25.190	17.91	18850.	157690.
3-332U	76.063	23.164	17.78	18464.	158231.
3-332F	73.996	27.236	17.91	17942.	154375.
3-113U	81.946	8.636	18.16	18050.	168666.
3-113F	81.328	9.729	18.16	18090.	167797.
3-213U	82.139	11.312	17.65	19133.	168752.
3-213F	80.520	14.006	17.65	19454.	167210.

SAMPLE DESIG.	DENSITY (LB/FT3)	MC (%)	HEIGHT (CM)	STANDARDIZED AM(CPM)	CS(CPM)
3-313U	82.718	11.554	17.65	18033.	166109.
3-313F	81.648	12.346	17.78	18099.	165596.
3-123U	84.113	12.258	18.16	12675.	151725.
3-123F	82.233	15.000	18.16	13136.	150924.
3-223U	82.322	17.465	18.03	12258.	146520.
3-223F	81.398	18.001	18.03	12985.	148260.
3-323U	80.582	18.855	18.16	12756.	146987.
3-323F	80.616	18.220	18.16	13088.	148396.
3-133U	81.176	29.567	18.03	7849.	123521.
3-133F	81.559	30.541	17.91	7628.	122073.
3-233U	79.456	33.713	18.03	7697.	120657.
3-233F	80.580	31.731	18.03	7539.	121058.
3-333U	77.867	36.462	18.03	7978.	120375.
3-333F	80.282	32.391	17.91	7933.	122312.